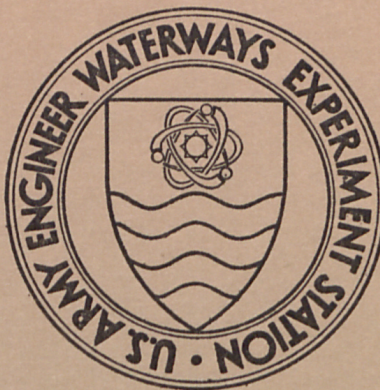


TA7
W34m
no.S-70-8
rept.2
c.4

NORTH
U.S. ARMY
DIVISION
CORPS OF ENGINEERS



MISCELLANEOUS PAPER S-70-8

EFFECTS OF STRAIN RATE IN CONSOLIDATED-UNDRAINED TRIAXIAL COMPRESSION TESTS OF COHESIVE SOILS

Report 2

VICKSBURG BUCKSHOT CLAY (CH)

by

R. T. Donaghe



May 1971

Sponsored by Office, Chief of Engineers, U. S. Army

Conducted by U. S. Army Engineer Waterways Experiment Station, Vicksburg, Mississippi



MISCELLANEOUS PAPER S-70-8

EFFECTS OF STRAIN RATE IN CONSOLIDATED-UNDRAINED TRIAXIAL COMPRESSION TESTS OF COHESIVE SOILS

Report 2

VICKSBURG BUCKSHOT CLAY (CH)

by

R. T. Donaghe



May 1971

Sponsored by Office, Chief of Engineers, U. S. Army

Conducted by U. S. Army Engineer Waterways Experiment Station, Vicksburg, Mississippi

ARMY-MRC VICKSBURG, MISS.

APPROVED FOR PUBLIC RELEASE; DISTRIBUTION UNLIMITED

Foreword

The investigation reported herein is part of a continuing evaluation of laboratory testing procedures for the Office, Chief of Engineers (OCE), under Item ES 516 of the Engineering Studies Program. Authorization for the testing program was given by OCE 1st Ind dated 5 December 1968 to U. S. Army Engineer Waterways Experiment Station (WES) letter, WESSE, dated 26 November 1968, subject: Proposed Research Program on Effect of Strain Rate on Strength of Compacted Fat Clay. The test program was completed during the period August 1969 through February 1970. This report is the second in a series of data reports on the effect of strain rate in R triaxial compression tests. Report 1 on Vicksburg silty clay (CL) was published as MP S-70-8 in February 1970.

The tests were conducted and the report was prepared by Mr. R. T. Donaghe, Laboratory Research Section, Embankment and Foundation Branch, Soils Division, under the supervision of Mr. B. N. MacIver, former Chief, Laboratory Research Section, and the general direction of Mr. J. R. Compton, Chief, Embankment and Foundation Branch, and Messrs. J. P. Sale and R. G. Ahlvin, Chief and Assistant Chief, respectively, Soils Division.

COL Levi A. Brown, CE, and COL Ernest D. Peixotto, CE, were Directors of WES during the preparation of this report. Mr. F. R. Brown was Technical Director.

Contents

	<u>Page</u>
Foreword	iii
Conversion Factors, British to Metric Units of Measurement. . . .	vii
Summary	ix
Introduction	1
Description of Soil and Testing Program	2
Description of Equipment	2
Preparation of Specimens	5
Testing Procedures	7
Saturation	7
Consolidation	8
Test Results	9
Specimen properties	9
Deviator stresses	16
Induced pore pressures	21
Effective stresses	25
Influence of specimen deformation on deviator stresses . .	30
Strength envelopes	37
Summary and Conclusions	40

Conversion Factors, British to Metric Units of Measurement

British units of measurement used in this report can be converted to metric units as follows:

<u>Multiply</u>	<u>By</u>	<u>To Obtain</u>
inches	25.4	millimeters
pints (U. S. liquid)	0.4731765	cubic decimeters
pounds	0.45359237	kilograms
pounds per cubic foot	16.0185	kilograms per cubic meter

Summary

The results of consolidated-undrained (R) triaxial compression tests with pore pressure measurements performed to determine the effects of strain rate on the strength and deformation characteristics of Vicksburg buckshot clay (CH) are presented and analyzed in this report. The 1.4-in.-diam triaxial specimens were compacted with a Harvard miniature compactor to 95 percent of maximum dry density derived from the standard effort compaction test with water contents 2 percentage points wet of standard optimum. Standard caps and bases (having the same diameter as the test specimen, with 1-in.-diam rigid porous inserts and drainage connections) were used in the triaxial tests. After back-pressure saturation and consolidation under effective confining pressures of 0.5 and 5.0 kg per sq cm, specimens with and without filter strips were axially loaded at rates of strain varying from 1.2 to 0.0012 percent per minute. Data presented include stress-strain curves, pore pressure observations, final water content distributions within the specimens, and shear strength envelopes based on total stresses.

The use of filter strips on the sides of the specimens appreciably reduced times required for saturation of all specimens and for consolidation of specimens under the effective pressures ($\bar{\sigma}_c$) of 5.0 kg per sq cm.

Using the normal procedures for calculating deviator stresses, deviator stresses at failure were lowest at rates of strain of 0.012 and 0.12 percent per min for tests at $\bar{\sigma}_c = 0.5$ and 5.0 kg per sq cm, respectively. Times to failure for the two $\bar{\sigma}_c$ were similar (133 and 125 min, respectively). Specimens sheared under $\bar{\sigma}_c = 0.5$ kg per sq cm failed at axial strains ranging between 1 and 3 percent; specimens sheared under $\bar{\sigma}_c = 5.0$ kg per sq cm continued to have increasing deviator stress with increasing axial strain. Very localized bulging of specimens occurred in tests at the two slowest rates of strain; this bulging or barreling invalidates the assumption that the specimen remains cylindrical for its entire height during axial loading. The conventional method for computing specimen area at large axial strains is not applicable for specimens that exhibit excessive bulging. The use of low-friction caps and bases to reduce end restraint and minimize the tendency of some specimens to exhibit a bulging failure mode will be investigated, and results will be presented in a subsequent report.

A modified method for computing specimen area during axial loading to take in account excessive bulging is discussed.

EFFECTS OF STRAIN RATE IN
CONSOLIDATED-UNDRAINED TRIAXIAL COMPRESSION TESTS OF COHESIVE SOILS

Report 2

VICKSBURG BUCKSHOT CLAY (CH)

Introduction

1. The present practice of the Corps of Engineers, as set forth in EM 1110-2-1906,* is to perform the consolidated-undrained triaxial compression test, termed R test in Corps of Engineers nomenclature, by first completely saturating each of at least three identical soil specimens and isotropically consolidating each specimen under a different effective pressure. Then drainage connections to the specimen are closed and the specimen is compressed to at least 15 percent axial strain. Pore water pressures developed during shear are not generally measured in routine testing.

2. Since R triaxial tests are time-consuming and expensive, it is highly desirable that procedures used by the Division laboratories be as economical as possible. An important element of the testing procedure is the time to failure or duration of the axial loading phase to the maximum deviator stress. From 1965 to 1970, time to failure was specified to be between 60 and 120 min for cohesive soil. For tests in which it was desired to develop stress-strain curves to 15 percent strain and where maximum deviator stress is reached at low strains, this procedure was time-consuming. For example, if a constant strain rate is used during shear and maximum deviator stress occurs at 3 percent strain, some clay samples are sheared for 120 min to reach this peak stress. If the test is carried to 15 percent strain, about 8 hr more would be required to complete the test. The purpose of this investigation is to determine the rate of strain in the R test that will give the lowest value for maximum deviator stress so that the most conservative total stress envelope can be developed.

* Department of the Army, Office, Chief of Engineers, "Engineering and Design: Laboratory Soils Testing," Engineer Manual EM 1110-2-1906, 30 November 1970, Washington, D. C.

Description of Soil and Testing Program

3. For this investigation, R tests were performed on 1.4-in.*-diam by 3-in.-high specimens of Vicksburg buckshot clay (CH) (standard soil sample) compacted to 95 percent of standard maximum dry unit weight at a water content 2 percent above standard optimum water content. Some properties of the Vicksburg buckshot clay are**:

Liquid limit	56
Plastic limit	22
Plasticity index	34
Percent finer than 2 μ	39
Standard maximum dry unit weight, pcf	97.8
Standard optimum water content, %	22.5

Moisture-density relationships are shown in fig. 1.

4. The R tests were performed to determine time-strength relationships for specimens both with and without filter strips. Specimens were fully saturated by back pressure and consolidated under effective pressures of 0.5 and 5.0 kg per sq cm. Nominal rates of strain of 1.2, 0.12, 0.012, and 0.0012 percent per minute were used to determine the undrained shear strength. Pore pressures during shear were measured at the bottom of the specimens. The final water content distribution within each specimen was determined by cutting the specimen horizontally into seven slices after shear.

Description of Equipment

5. A schematic diagram of the testing apparatus is shown in fig. 2,

* A table of factors for converting British units of measurement to metric units is presented on page vii.

** W. E. Strohm, Jr., "Preliminary Analysis of Results of Division Laboratory Tests on Standard Soil Samples," MP No. 3-813, April 1966, U. S. Army Engineer Waterways Experiment Station, CE, Vicksburg, Miss.

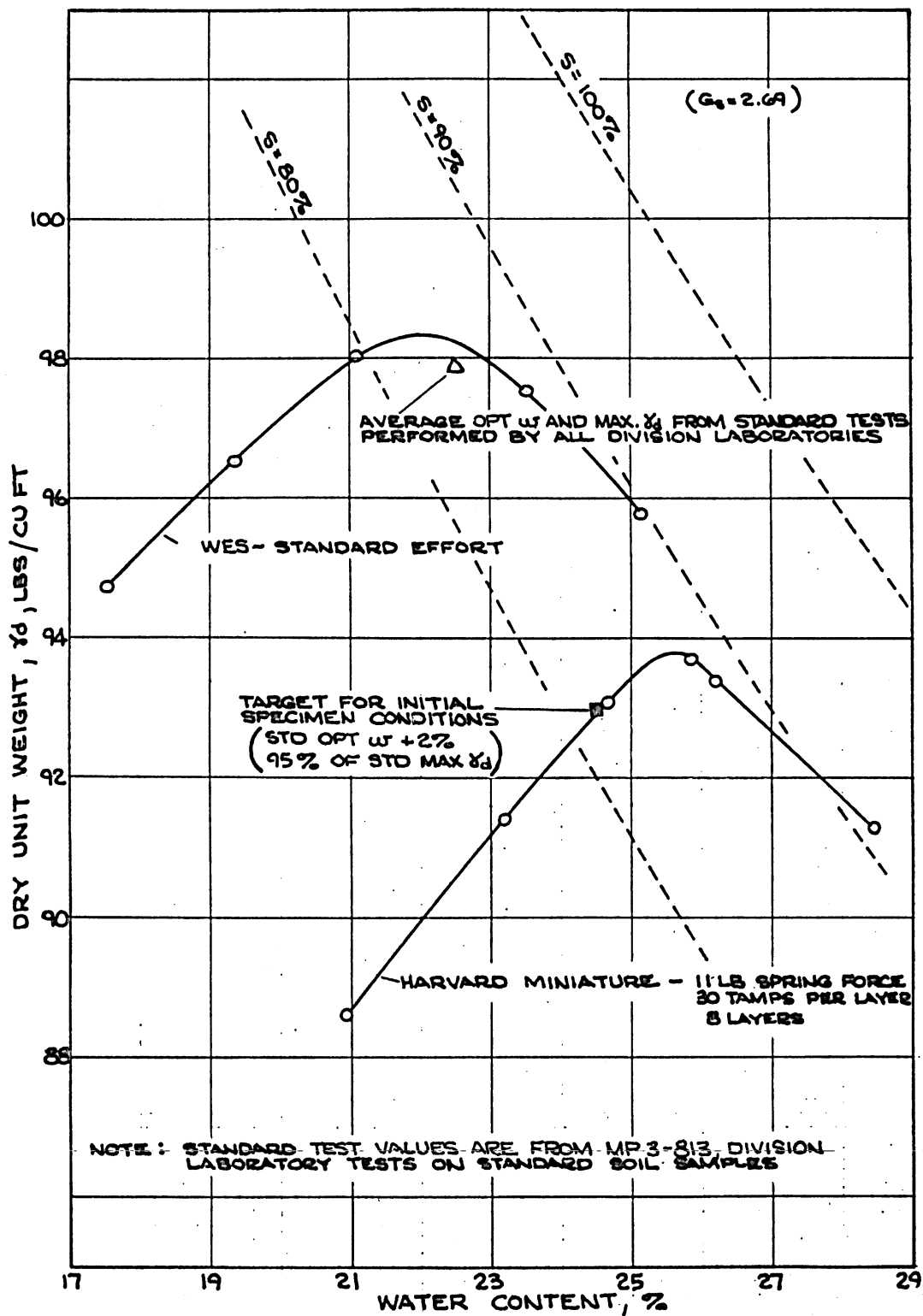


Fig. 1. Moisture-density relationships for Vicksburg buckshot clay

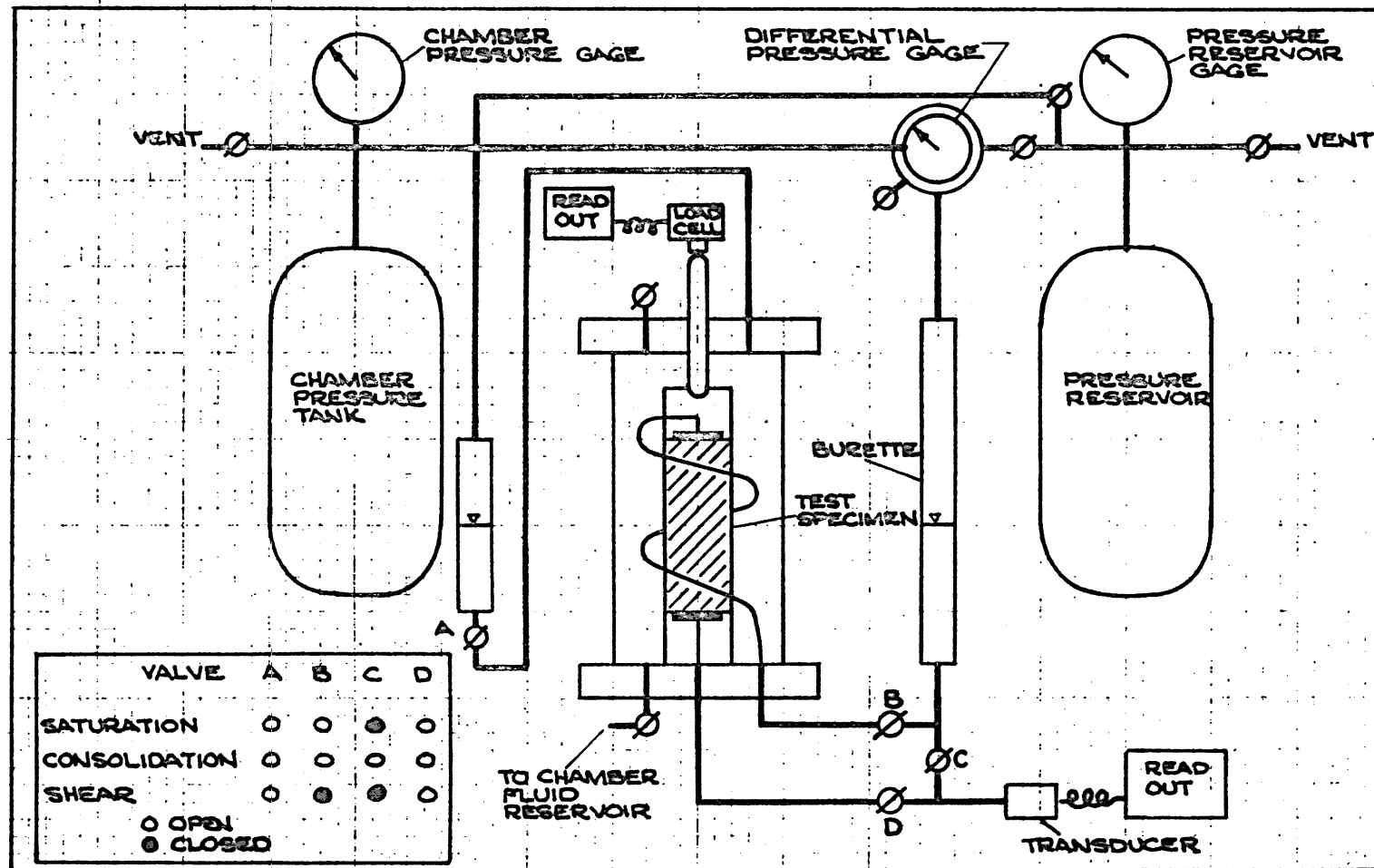


Fig. 2. Schematic diagram of testing apparatus

and a photograph has been included as fig. 3. The triaxial chambers with specimen bases and caps and axial loading pistons were those used regularly in the U. S. Army Engineer Waterways Experiment Station (WES) Soils Laboratory for Division soil testing.* A closed system of pressurized nitrogen gas was used to apply the confining and back pressures. These pressures were manually adjusted with needle valves and were measured with Bourdon tube gages. Pore water pressure was measured at the base of each specimen using an electronic pressure transducer, while an electronic load cell was used to measure the force applied to the piston. Transducers, load cells, and gages were calibrated so that all pressures and stresses were accurate to 0.01 kg per sq cm. Changes in height of each specimen were measured with a dial indicator reading 0.01 mm per division. Tap water was used for the chamber fluid, and distilled water was used to saturate the specimen. The volume of water entering and leaving the specimen during saturation and consolidation was measured with a calibrated burette. Whatman No. 1 chromatography paper was used for the filter strips.

Preparation of Specimens

6. The desired initial specimen conditions, based on standard compaction tests, were a water content 2 percent above optimum water content and a dry unit weight equal to 95 percent of maximum dry unit weight; this required an as-compacted water content of 24.5 percent and a dry unit weight of 93.0 pcf. Batches for individual specimens were prepared in a humid room by mixing a previously weighed amount of air-dried soil with sufficient distilled water to obtain the desired water content. After mixing, each batch was placed in an airtight 1/2-pint glass jar and allowed to cure for at least 7 days.

7. All specimens were compacted to the desired dry unit weight in the humid room using a Harvard miniature compactor having a spring that gave a tamping force of approximately 11 lb. The diameter of the tamping foot was 1/2 in. Each specimen was compacted in a 4-piece, 1.4-in.-diam

* Op. cit., EM 1110-2-1906, Appendix X, fig. 2.

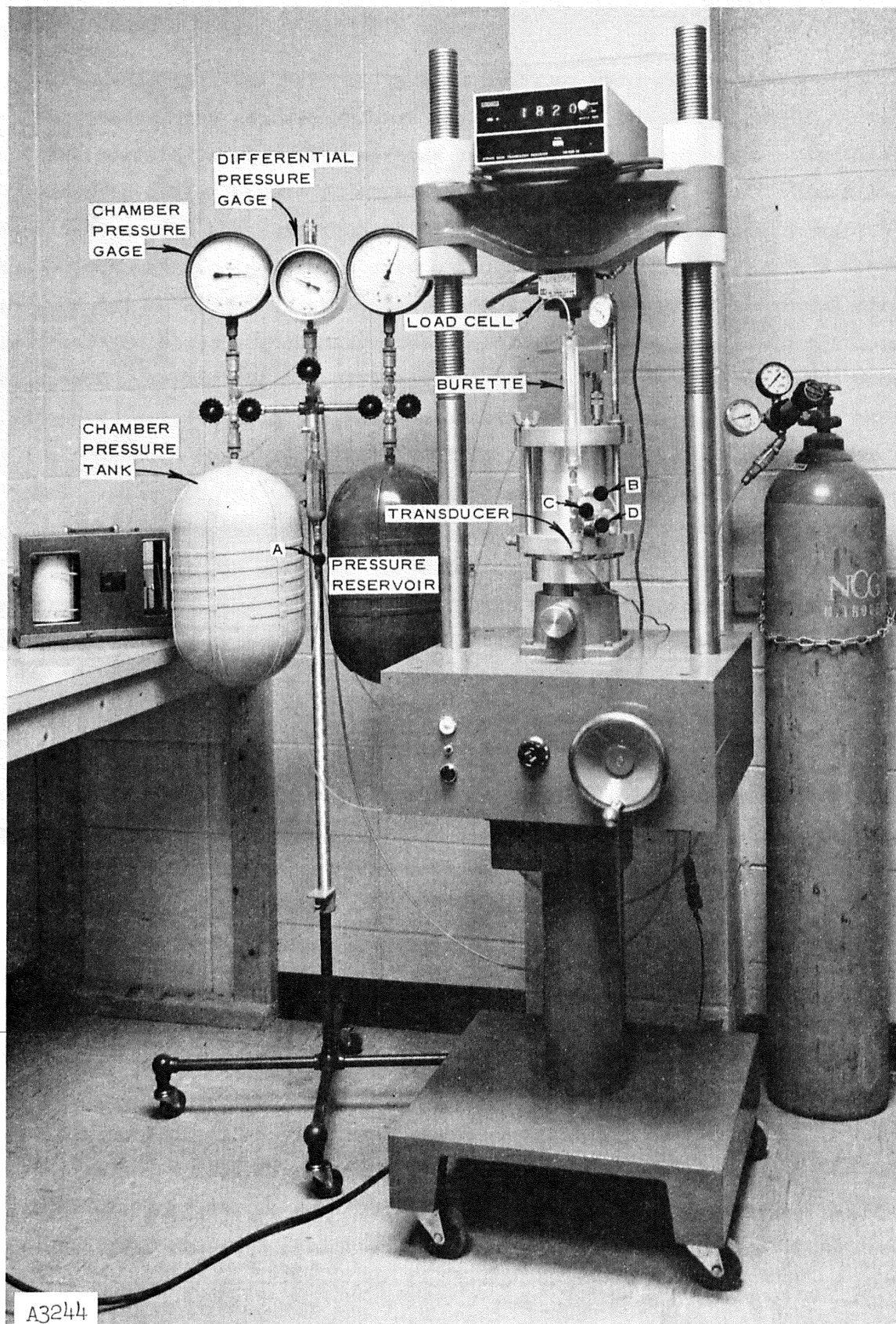


Fig. 3. Testing apparatus

by 3.0-in.-high mold in eight layers using 30 tamps (three complete coverages of the surface area) on each layer. Approximately one-half of the last layer was trimmed away to obtain the desired 3.0-in. specimen height. After the sides of the mold were stripped away and the wet weight of the specimen was checked, each specimen (including filter strips when applicable) was covered with two standard 0.012-in.-thick rubber membranes and placed in a triaxial chamber. The specimen cap and base were 1.4 in. in diameter and made of lucite with rigid porous inserts. The membranes were sealed at the cap and base using two O-rings at each end.

8. When filter strips were used, they were evenly spaced around the perimeter of the specimen and extended from the top porous stone to slightly more than 0.7 in. from the bottom edge of the specimen. Six strips were used. Fifty percent of the specimen perimeter was covered by the strips.

Testing Procedures

Saturation

9. All specimens were initially subjected to a differential pressure of 0.25 kg per sq cm (chamber pressure minus back pressure) with access to water at both top and bottom. After burette readings indicated an equilibrium condition had been reached, the valve between the burette and the bottom of the specimen (valve C of fig. 2) was closed and the chamber pressure and back pressure were increased by increments of 0.25 kg per sq cm, thus maintaining a differential pressure of 0.25 kg per sq cm at the top of the specimen. The rate at which increments were added was such that the differential pressure at the bottom of the specimen (chamber pressure minus pressure indicated by the pore pressure transducer) never exceeded 0.5 kg per sq cm. A total back pressure of 8 kg per sq cm was used to saturate each specimen. The time for complete saturation averaged 12 days for specimens without filter strips and 4 days for specimens with strips. Prior to initiating consolidation, the pore pressure parameter B was measured by closing the valve to the top of the specimen and raising the chamber pressure by several increments of 0.1 kg per sq cm while observing

the corresponding pore pressure response. If the pore pressure response was immediate and corresponded to the increase in chamber pressure, consolidation was initiated.

Consolidation

10. After reading the vertical height dial indicator, the differential pressure (chamber pressure minus back pressure) was increased to the desired effective consolidation pressure. Valves to the top and bottom of the specimen were then opened, allowing water from the specimen to enter the burette. Burette readings were taken at time intervals such that a semi-logarithmic plot of the volume of water draining from the specimen versus time could be made. Each specimen was consolidated for at least 24 hr after completion of primary consolidation. Consolidation time for specimens consolidated under an effective pressure of 0.5 kg per sq cm averaged 3 days, both with and without filter strips. For those specimens consolidated under an effective pressure of 5.0 kg per sq cm, the time for consolidation averaged 6 days without filter strips and 4 days with strips. Times for 50 percent primary consolidation computed for the tests at 5.0 kg per sq cm averaged 375 min for specimens without filter strips and 23 min for specimens with strips. For the 5.0-kg-per-sq-cm tests, the ratio between the coefficient of consolidation with strips and the coefficient of consolidation without strips was 3.5.

11. Upon completion of consolidation, the valves to the top and bottom of the specimen were closed and the vertical height indicator was read. The specimen was then axially loaded at a constant rate of strain. When the specimen had been deformed to 20 percent axial strain, the test was stopped and the chamber pressure was removed, with the valves to the top and bottom of the specimen remaining closed. The compression chamber (including the transducer and valves) was then quickly moved to the humid room where the drainage lines to the top and bottom of the specimen were disconnected. The membranes inclosing the specimen were then removed and the specimen was cut into seven horizontal slices. The height of the top and bottom slices was half that of each of the five central slices. Water contents of the five central slices were then determined. Water contents of the top and bottom slices were not determined since they might have acquired water from the porous stones when the lines to the specimen were

disconnected. The zero readings of the load cell and transducer were checked at the end of the test.

Test Results

12. Results for a total of 17 tests are summarized in tables 1 and 2 and presented graphically in figs. 4 through 20. The tests are grouped in the tables and figures according to effective consolidation pressure. Tests 1 through 8 were performed under effective consolidation pressures of 0.5 kg per sq cm, and tests 9 through 17 were performed under effective consolidation pressures of 5.0 kg per sq cm. The results are discussed under the following headings:

- a. Specimen properties
- b. Deviator stresses
- c. Induced pore pressures
- d. Effective stresses
- e. Influence of specimen deformation on deviator stresses
- f. Strength envelopes

Specimen properties

13. As compacted. Data indicating as-compacted specimen conditions are listed in table 1. As-compacted water contents varied from 24.4 to 25.3 percent and dry unit weights ranged from 91.8 to 93.9 pcf. Average values for these water contents and dry unit weights were 24.8 percent and 92.8 pcf, respectively. This compares to the desired as-compacted water content and dry unit weight values of 24.5 percent and 93.0 pcf, respectively. It should be noted that the desired 24.5 percent water content plots somewhat on the dry side of the Harvard miniature curve as shown in fig. 1.

14. After consolidation. Specimen conditions after consolidation given in table 1 indicate the following changes in water content and dry

Table 1
Summary of Data Prior to Axial Loading

Test No.	Nominal Rate of Strain %/min	As-Compacted Conditions								Conditions After Consolidation	
		Water Content w, %	Void Ratio e	Degree of Saturation s, %	Dry Unit Weight γ_d , pcf	Saturation Period		Consolidation Period		Water Content* %	Dry Unit Weight** γ_d , pcf
						min	days	min	days		
Effective Consolidation Pressure, $\bar{\sigma}_c = 0.5 \text{ kg/cm}^2$											
Without Filter Strips											
1	1.2	25.2	0.80	85	93.4	18,720	13.0	4,034	2.8	29.8	93.2
2	0.12	25.1	0.82	82	91.8	17,476	12.1	3,909	2.7	31.2	91.2
3	0.012	25.3	0.83	82	91.8	15,650	10.9	2,845	2.0	30.3	92.4
4	0.0012	24.9	0.83	80	93.0	17,180	11.9	2,801	1.9	29.8	93.1
						Avg	12.0		2.4		
With Filter Strips											
5	1.2	25.0	0.82	82	92.0	8,233	6.7	2,779	1.9	30.8	91.7
6	0.12	24.8	0.81	82	92.4	2,663	1.8	4,233	2.9	30.2	92.6
7	0.012	24.9	0.81	83	92.9	4,118	2.9	5,694	3.9	30.0	92.8
8	0.0012	24.8	0.82	81	92.2	5,407	3.8	4,415	3.1	30.9	91.6
						Avg	3.8		2.9		
Effective Consolidation Pressure, $\bar{\sigma}_c = 5.0 \text{ kg/cm}^2$											
Without Filter Strips											
9	1.2	24.8	0.80	83	93.1	17,074	11.8	9,982	6.9	23.1	103.5
10	0.12	24.6	0.79	84	93.9	15,330	10.6	10,220	7.1	23.3	103.1
11	0.012	24.4	0.79	83	93.8	18,533	12.8	8,517	5.9	23.3	103.3
12	0.0012	24.6	0.80	82	93.4	18,465	12.8	8,575	6.0	23.6	102.7
						Avg	12.0		6.5		
With Filter Strips											
13	1.2	24.7	0.81	82	92.6	7,849	5.4	2,869	2.0	22.9	103.9
14	0.12	25.0	0.82	82	91.8	5,409	3.7	2,888	2.0	23.1	103.6
15	0.012	24.7	0.80	83	93.3	3,947	2.7	5,716	4.0	23.0	104.3
16	0.0012	24.7	0.80	83	93.3	4,109	2.9	5,745	4.0	23.1	103.5
17	0.0012†	24.8	0.80	83	93.2	7,034	4.9	10,055	7.0	23.3	103.2
						Avg	3.9		3.8		

Note: A total back pressure of 8 kg/sq cm was used to saturate each specimen.

* Average after-test water content based on middle 83% of specimen

** Based on average after-test water content.

† Test to determine effect of additional time of consolidation.

Table 2
Summary of Axial Loading Data

Test No.	Nominal Rate of Strain %/min	At Max $\frac{\bar{\sigma}_1}{\bar{\sigma}_3}$							At Max $(\sigma_1 - \sigma_3)^*$						
		$\sigma_1 - \sigma_3$	$\mu - \mu_0$	$\bar{\sigma}_3$	$\frac{\bar{\sigma}_1}{\bar{\sigma}_3}$	A = $\frac{\mu - \mu_0}{\sigma_1 - \sigma_3}$	Strain $\epsilon, \%$	Time of Loading min	$\sigma_1 - \sigma_3$	$\mu - \mu_0$	$\bar{\sigma}_3$	$\frac{\bar{\sigma}_1}{\bar{\sigma}_3}$	A = $\frac{\mu - \mu_0}{\sigma_1 - \sigma_3}$	Strain $\epsilon, \%$	Time of Loading min
		kg/cm ²	kg/cm ²	kg/cm ²					kg/cm ²	kg/cm ²	kg/cm ²				
		Effective Consolidation Pressure, $\bar{\sigma}_c = 0.5$ kg/cm ²													
Without Filter Strips															
1	1.2	0.85	0.45	0.05	17.37	0.53	1.0	> 1	0.84	0.43	0.07	13.40	0.51	0.7	< 1
2	0.12	0.55	0.36	0.14	4.86	0.67	1.4	12	0.56	0.32	0.18	4.08	0.58	0.7	6
3	0.012	0.52	0.32	0.18	3.90	0.61	1.6	133	0.54	0.31	0.19	3.33	0.57	1.0	85
4	0.0012	0.53	0.29	0.21	3.67	0.57	2.3	1,918	0.54	0.29	0.21	3.58	0.55	1.6	1,359
With Filter Strips															
5	1.2	0.66	0.40	0.10	7.56	0.61	1.4	1	0.68	0.37	0.13	6.16	0.54	0.7	< 1
6	0.12	0.57	0.34	0.16	4.49	0.60	1.8	15	0.57	0.33	0.17	4.43	0.58	1.2	10
7	0.012	0.52	0.32	0.18	3.86	0.61	3.8	317	0.50	0.32	0.18	3.76	0.64	1.6	133
8	0.0012	0.52	0.31	0.19	3.73	0.60	3.5	2,920	0.51	0.32	0.18	3.71	0.63	2.1	2,742
Effective Consolidation Pressure, $\bar{\sigma}_c = 5.0$ kg/cm ²															
Without Filter Strips															
9	1.2	3.83	3.76	1.24	4.08	0.98	15.0	13	3.83	3.76	1.24	4.09	0.98	15	13
10	0.12	3.56	3.23	1.77	2.88	0.90	13.7	114	3.58	3.21	1.79	2.87	0.90	15	125
11	0.012	3.53	2.98	2.02	2.73	0.84	9.6	800	3.66	2.73	2.27	2.61	0.74	15	1,250
12	0.0012	3.61	2.70	2.30	2.58	0.76	10.6	8,833	3.68	2.60	2.40	2.54	0.69	15	12,500
With Filter Strips															
13	1.2	3.95	3.56	1.44	3.74	0.90	15.0	13	3.94	3.56	1.44	3.74	0.90	15	13
14	0.12	3.73	3.06	1.94	2.92	0.82	12.4	103	3.78	3.02	1.98	2.92	0.79	15	125
15	0.012	3.67	2.83	2.17	2.69	0.77	7.7	644	3.95	2.50	2.50	2.56	0.63	15	1,250
16	0.0012	3.99	2.58	2.42	2.65	0.65	8.4	7,120	4.26	2.25	2.75	2.56	0.54	15	12,500
17**	0.0012	4.09	2.51	2.49	2.64	0.61	8.7	7,237	4.31	2.29	2.71	2.60	0.54	15	12,500

Note: Symbols used in the headings are defined in EM 1110-2-1906.

* Maximum deviator stresses (a) for tests at $\bar{\sigma}_c = 0.5$ kg/sq cm were taken at the initial yield (see fig. 7), (b) for tests at $\bar{\sigma}_c = 5.0$ kg/sq cm were taken at 15 % strain (see fig. 9); deviator stresses were computed using customary area corrections.

** Test to determine effect of additional time of consolidation.

unit weight prior to shear:

End of Consolidation Minus As-Compacted Values				
	w, %		γ_d , pcf	
	Range	Avg	Range	Avg
1. $\bar{\sigma}_c = 0.5$ kg/sq cm:				
a. Without filter strips (tests 1-4)	+ 4.6 to + 6.1	+ 5.2	- 0.6 to + 0.6	0
b. With filter strips (tests 5-8)	+ 5.1 to + 6.1	+ 5.6	- 0.6 to + 0.2	- 0.2
2. $\bar{\sigma}_c = 5.0$ kg/sq cm:				
a. Without filter strips (tests 9-12)	- 1.7 to - 1.0	- 1.3	+ 9.2 to + 10.4	+ 9.6
b. With filter strips (tests 13-17)	- 1.9 to 1.5	- 1.7	+ 10.0 to + 11.8	+ 10.8

The average dry unit weight prior to shear of specimens consolidated under an effective pressure of 5.0 kg per sq cm with filter strips was 1.2 pcf higher than those consolidated at the same pressure without strips. There was essentially no difference in the unit weights prior to shear for specimens with and without filter strips consolidated under an effective pressure of 0.5 kg per sq cm.

15. After testing. Final water content distributions and failure sketches of the specimens are given in figs. 4 and 5. The final water content distributions indicate that at least during the latter stages of shear, pore water generally migrated from the top portions of the specimens toward the center and bottom. This occurrence was apparently independent of the presence of filter strips and the magnitude of the effective consolidation pressure. The effect of rate of strain on pore water migration may be seen in fig. 6, a plot of the difference between the final water content of the center slice and average final specimen water content versus elapsed time of shear. The curves for the tests at 0.5 kg per sq cm show that the water content (and thus the void ratio) of the center portion of these test specimens increased

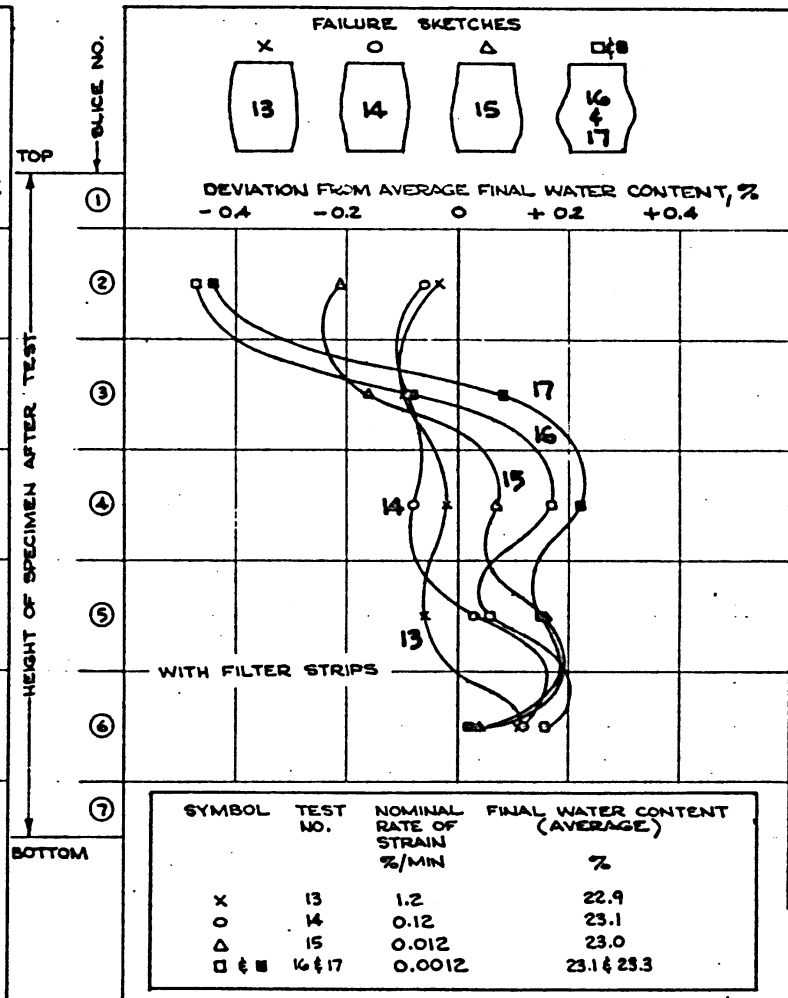
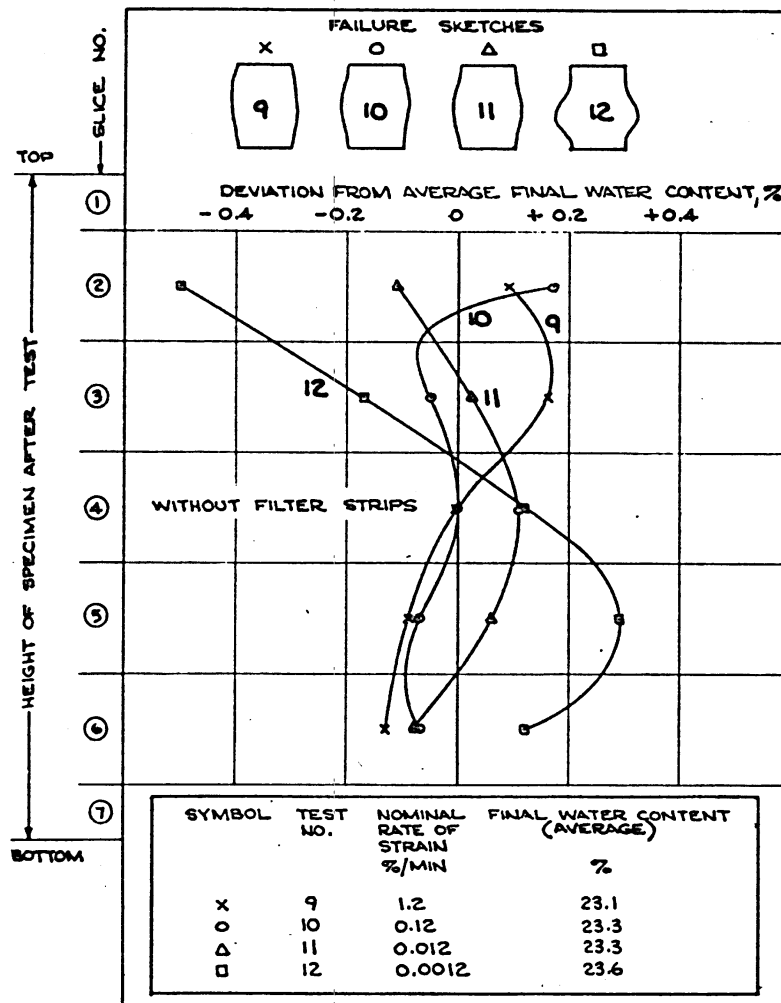


Fig. 5. Final water content distributions, $\bar{\sigma}_c = 5.0 \text{ kg/sq cm}$

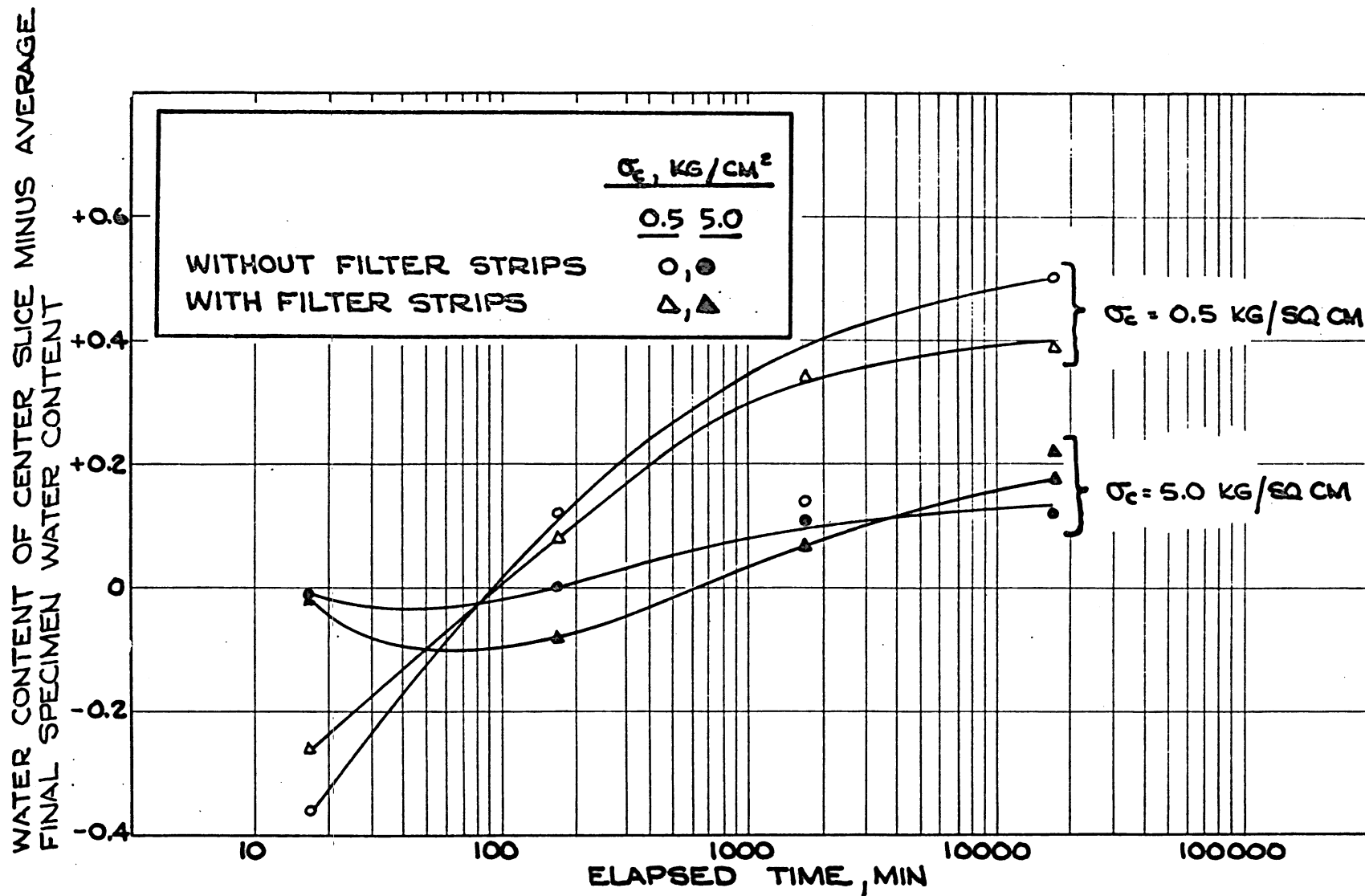


Fig. 6. Water content of center slice minus average final specimen water content versus elapsed time of shear

as the time of shear was increased. Since overconsolidated specimens usually attempt to dilate when sheared, this relationship was to be expected. The curves for the tests at 5.0 kg per sq cm show less increase in water content of the center with increased time of shear than the curves for the tests at 0.5 kg per sq cm. A possible explanation for this behavior may be seen in the failure sketches of fig. 5. All of the specimens failed by bulging; however, the bulging became more localized toward the center and bottom as the time of shear was increased. This is seen mainly as an effect of end restraint since, as the time of shear is increased, pore pressure gradients within the specimens dissipate and shear strains become more concentrated in the middle portion of the specimens. The increased shear deformation in this part of the specimens probably altered the soil structure sufficiently enough so that at large strains, an increase in void ratio occurred. When examining the water content distributions and failure sketches shown in these figures, one should keep in mind that these are final specimen conditions and may not be indicative of conditions during the initial stages of shear. Also it must be remembered that volume changes occurring within the specimen during saturation and consolidation as well as the possibility of nonuniform conditions in the as-compacted specimens would affect the final water content distribution. Finally, it is possible that removal of the failed specimen from the membrane and slicing it into sections altered the water content distribution compared to the end-of-shear condition.

Deviator stresses

16. Tests at $\bar{\sigma}_c = 0.5$ kg per sq cm. Stress-strain curves are shown in fig. 7. Deviator stresses peaked at low axial strains (0.7 to 2.1 percent) and then, after decreasing, began increasing gradually at strains of 2 to 6 percent to the end of the tests. The deviator stress at the initial peak of the stress-strain curve was selected as the deviator stress at failure. The apparent increase in deviator stress with further increase in strain is believed to reflect the inapplicability of the normal assumption made in correcting specimen areas to compute deviator stresses (this will be discussed later). Table 2 and fig. 7 show that for specimens both with and without filter strips, deviator stresses at

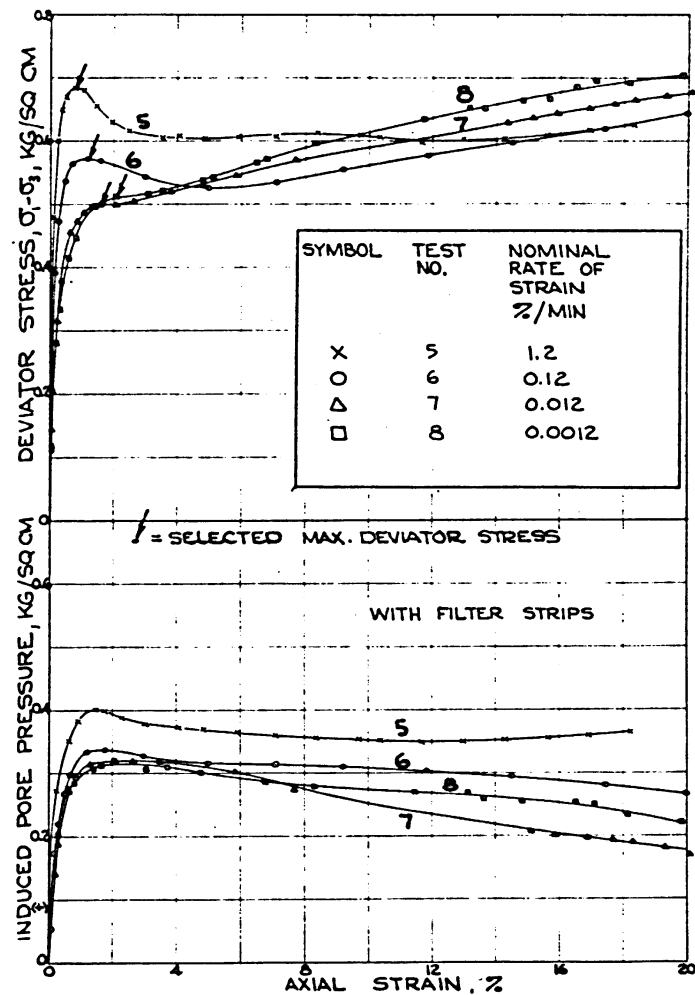
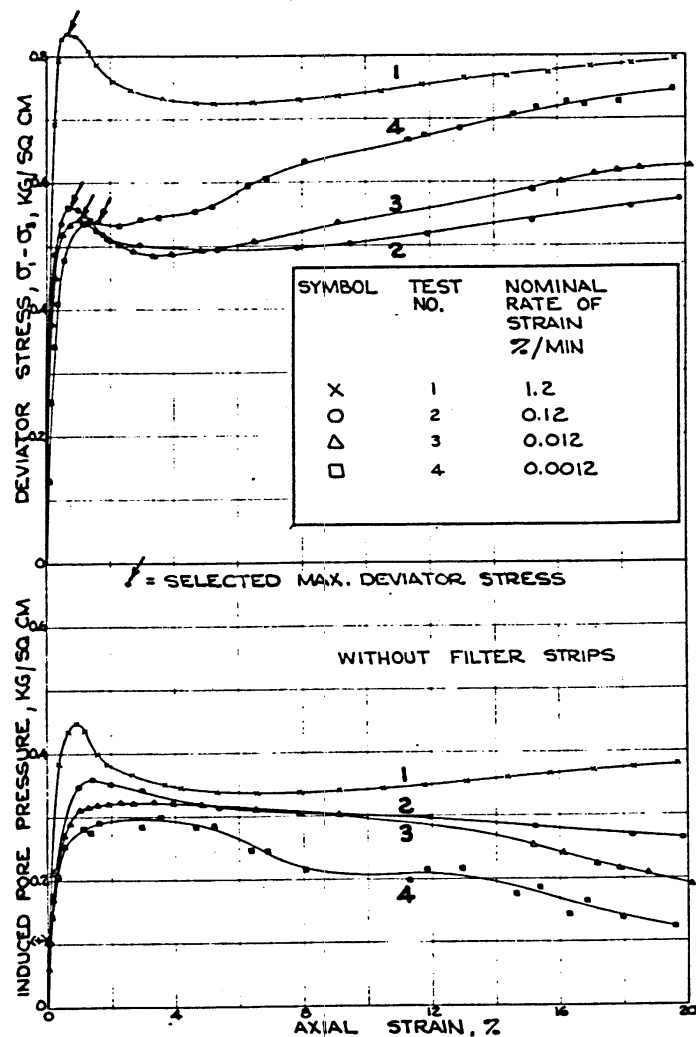


Fig. 7. Deviator stress and induced pore pressure versus axial strain,
 $\bar{\sigma}_c = 0.5$ kg/sq cm

failure decreased with decreasing rates of strain. Figure 8 is a plot of deviator stresses at failure and deviator stresses at 15 percent strain versus elapsed times of shear. The principal decrease occurred in reducing the rate of strain from 1.2 to 0.12 percent per min. The following tabulation shows the relative values of deviator stress at failure, taking the value obtained in tests at a rate of strain of 0.12 percent per min as 1:

	Rate of Strain, %/min			
	<u>1.2</u>	<u>0.12</u>	<u>0.012</u>	<u>0.0012</u>
<u>With filter strips:</u>				
Time to failure, min	< 1	10	133	1742
Deviator stress at failure relative to value at $\dot{\epsilon} = 0.12$ % per min	1.19	1.00	0.88	0.90
<u>Without filter strips:</u>				
Time to failure, min	< 1	6	85	1359
Deviator stress at failure relative to value at $\dot{\epsilon} = 0.12$ % per min	1.50	1.00	0.96	0.96

It is to be noted that the deviator stresses for tests conducted at 0.012 percent per min were 12 and 4 percent less than those at rates of strain of 0.12 percent per min for specimens with filter strips and without filter strips, respectively. There was practically no difference in deviator stresses in tests at the two slowest rates of strain. Curves of deviator stress at 15 percent strain shown in fig. 8 indicate that the deviator stresses increase in tests with rates of strain slower than 0.12 percent per min. This will be discussed later.

17. Tests at $\bar{\sigma}_c = 5.0$ kg per sq cm. Stress-strain curves are shown in fig. 9. All curves break rather sharply but without the peaks at low strains of tests at $\bar{\sigma}_c = 0.5$ kg per sq cm. Points of maximum curvature for the specimens without filter strips occurred at from 1.6 to 2.2 percent strain and those for specimens with filter strips occurred at from 1.7 to 3.6 percent strain. In general the deviator stress at the point of maximum curvature was approximately 80 percent of that at 15 percent strain. Both

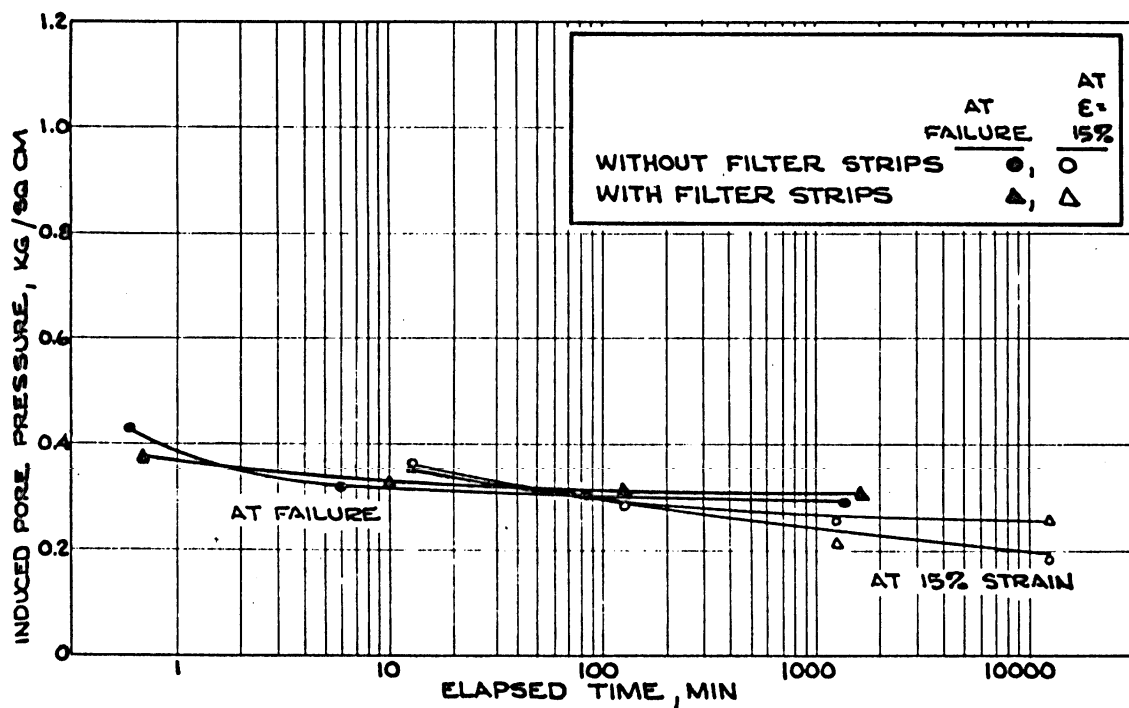
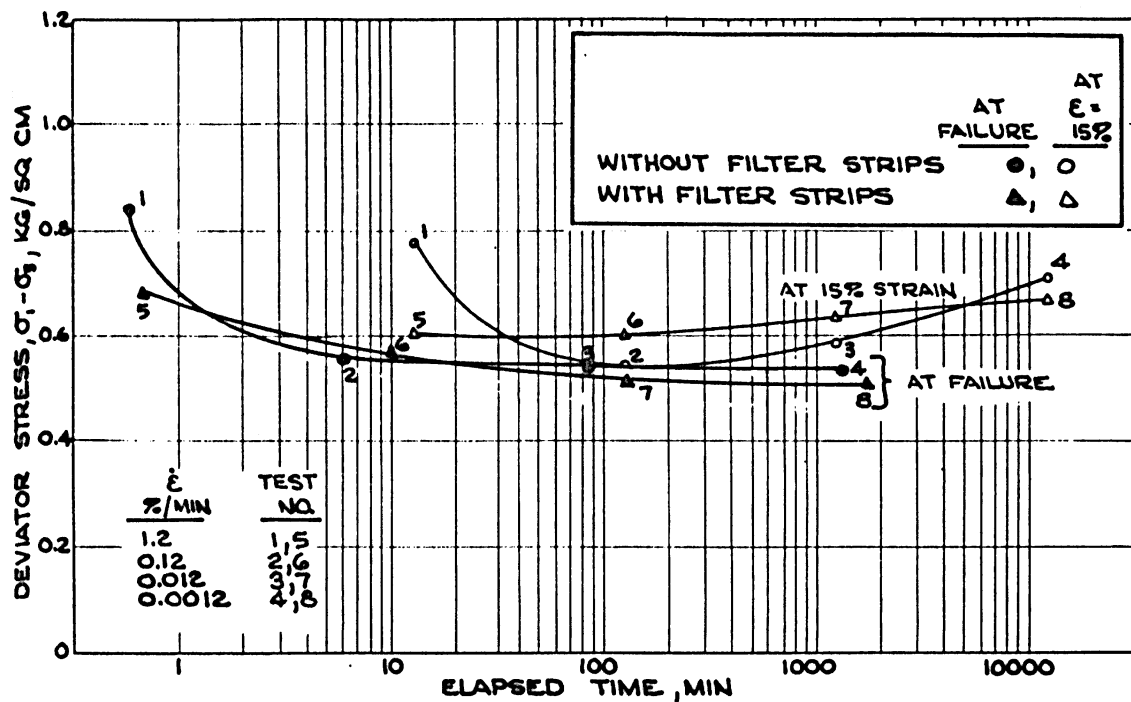


Fig. 8. Deviator stress and induced pore pressure versus elapsed times of shear at failure and at 15 percent axial strain, $\bar{\sigma}_c = 0.5$ kg/sq cm

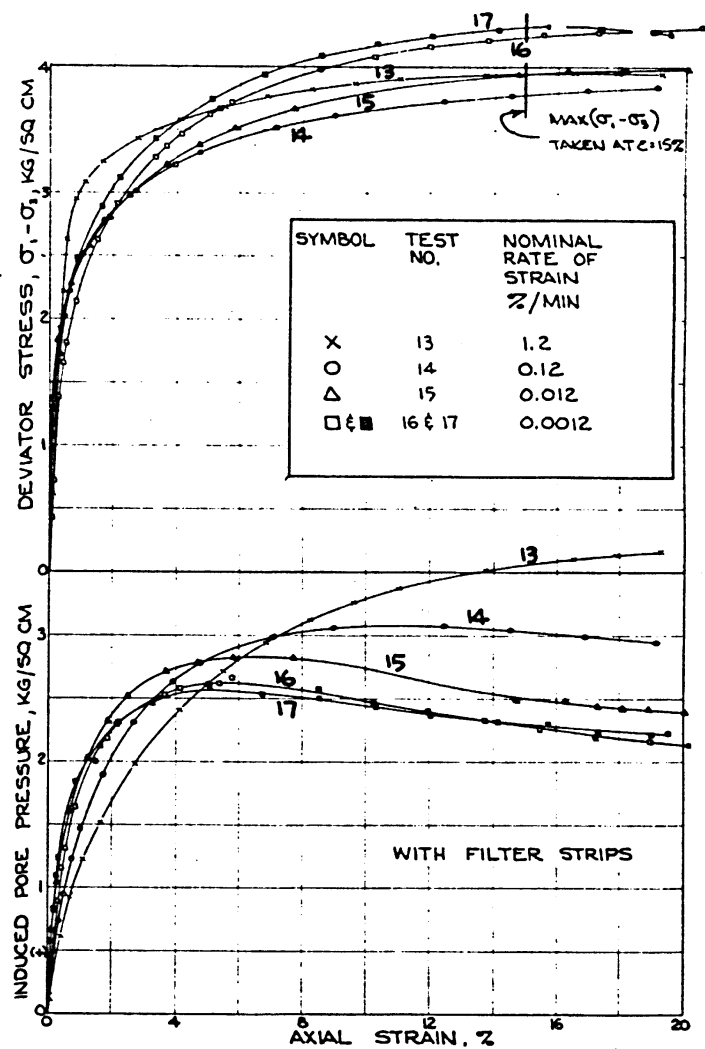
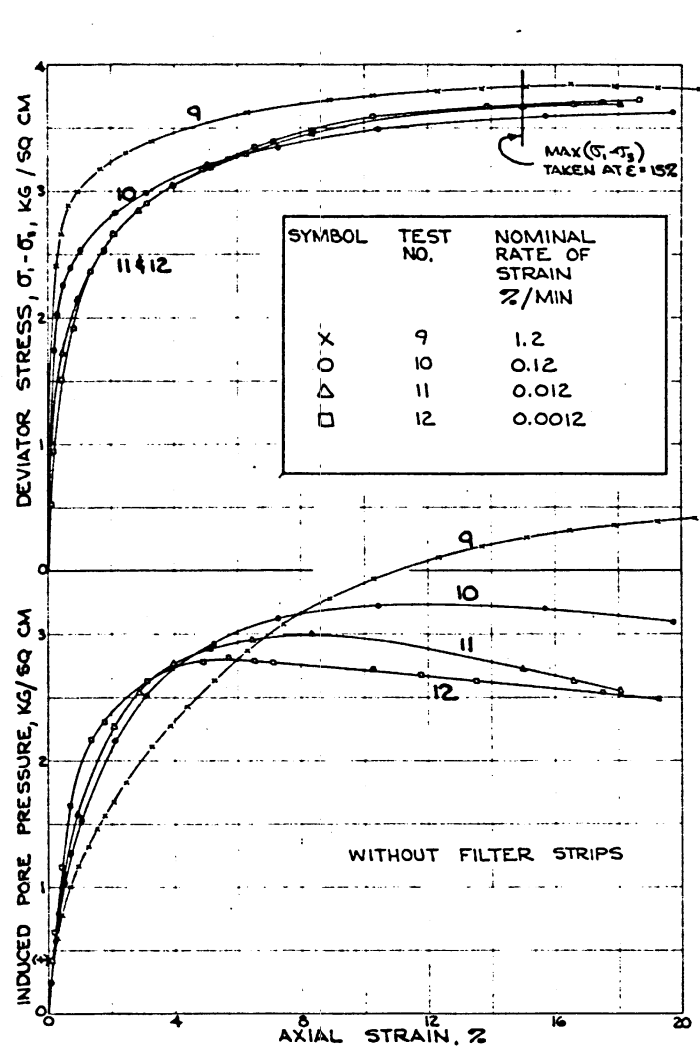


Fig. 9. Deviator stress and induced pore pressure versus axial strain, $\bar{\sigma}_c = 5.0$ kg/sq cm

deviator stress and axial strain values at the point of maximum curvature increased with increased times of shear. Plots of deviator stresses at 1 and 15 percent strain versus elapsed time of shear are given in fig. 10. This figure shows that deviator stresses at 1 percent strain decrease with decrease in rate of strain. The plots of deviator stresses at 15 percent strain (which is customarily taken as the maximum deviator stress in tests having stress-strain curves similar to those of these tests) show an apparent increase in deviator stress for the two slowest rates of strain. This is indicated by the following tabulation:

		Rate of Strain, %/min			
		1.2	0.12	0.012	0.0012
<u>With filter strips:</u>					
Time to 15 percent strain, min	13	125	1250	12,500	
Deviator stress at 15 percent strain relative to value at $\dot{\epsilon} = 0.12$ % per min	1.04	1.00	1.04	1.13	
<u>Without filter strips:</u>					
Time to 15 percent strain, min	13	125	1250	12,500	
Deviator stress at 15 percent strain relative to value at $\dot{\epsilon} = 0.12$ % per min	1.07	1.00	1.02	1.03	

The apparent increase in shear strength with slower rates of strain will be discussed later.

18. Tests 16 and 17 were sheared at the same rate (0.0012 %/min), after test 17 had been allowed to consolidate twice as long as test 16. The effect of the additional time for consolidation on the deviator stress at failure was shown to be negligible.

Induced pore pressures

19. 0.5-kg-per-sq-cm tests. Plots of pore pressure induced during shear versus axial strain for the 0.5-kg-per-sq-cm tests are shown in fig. 7. Induced pore pressures reached a maximum at between 1 and 3 percent strain, ranging from 0.30 to 0.45 kg per sq cm for specimens without filter strips and from 0.32 to 0.40 kg per sq cm for specimens with strips. Maximum pore pressures decreased with decreasing rates of

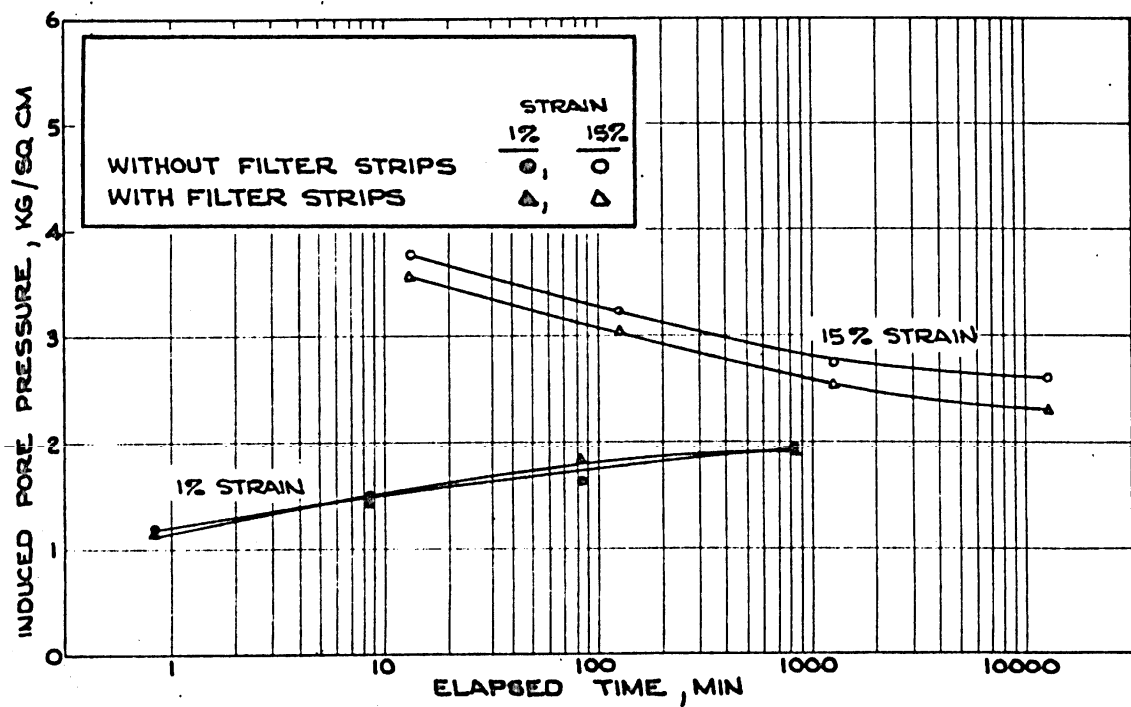
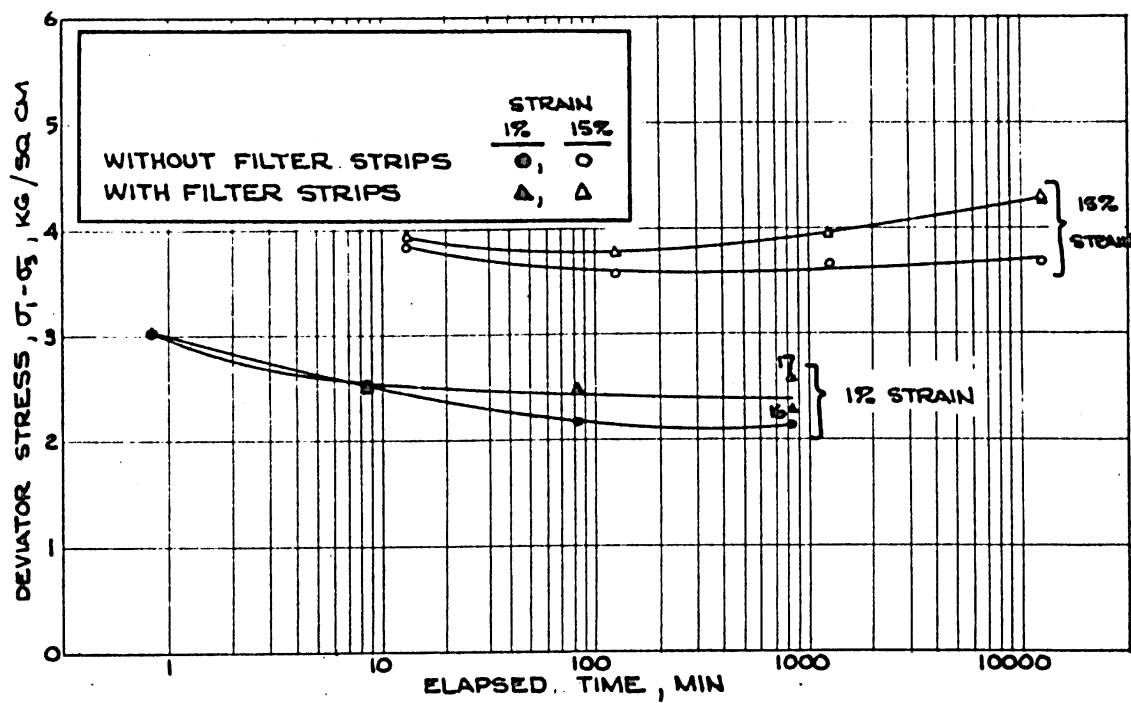


Fig. 10. Deviator stress and induced pore pressure versus elapsed times of shear at 1 and 15 percent strain, $\bar{\sigma}_c = 5.0$ kg/sq cm

strain, while the strains at which they developed increased. The relationship between induced pore pressure at failure and at 15 percent strain and the elapsed time of shear at these strain values, shown in fig. 8, indicates that induced pore pressure decreased with decreasing strain rates during both the initial and final stages of shear. The tabulation in paragraph 14 indicates that there was zero or very slight decrease in unit weight under consolidation pressure of 0.5 kg per sq cm, indicating that the compacted specimens were slightly overconsolidated relative to the test pressure. If the shear strains were predominant in the central portion of the specimen, there might be dilation of the central portion in which case, the pore water pressure would be lower in the middle than at the end where pore pressures were observed. Therefore, for the faster rates of strain, observed pore pressure would be higher than the average; while for slower rates of strain, with more time permitted for pore pressure equalization, the observed pore pressures would approach the average in the specimen. It is to be noted in fig. 8 that the curves of induced pore pressure versus time for tests with filter strips are somewhat flatter than those for tests without filter strips, perhaps indicating some benefit of filter strips in achieving pore pressure equalization. A plot of the A parameter (ratio of induced pore pressure to deviator stress) versus axial strain is given in fig. 11.

20. 5.0-kg-per-sq-cm tests. The relationships between induced pore pressure and axial strain for 5.0-kg-per-sq-cm tests are plotted in fig. 9. Induced pore pressures reached maximum values at axial strains ranging from 5 to 20 percent, and ranged from 2.80 to 3.90 kg per sq cm for specimens without filter strips and from 2.63 to 3.68 kg per sq cm for specimens with strips. Both the maximum pore pressures and the strains at which they developed decreased with decreasing rates of strain. It is interesting to note that the use of filter strips had no effect on the strain at which maximum induced pore pressure developed. Plots of induced pore pressure versus elapsed time of shear at axial strain values of 1 and 15 percent shown in fig. 10 show that pore pressures (which were measured at the bottom of the specimen) increased with decreasing strain rates during the initial part of shear and decreased with decreasing

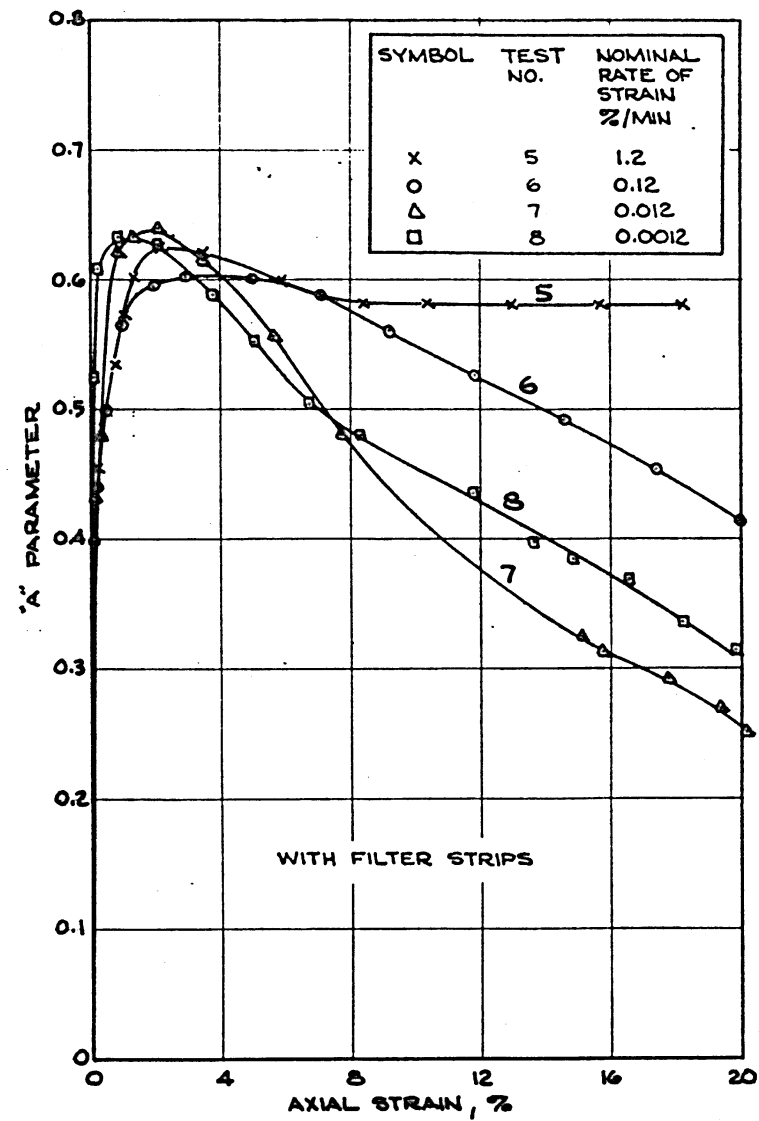
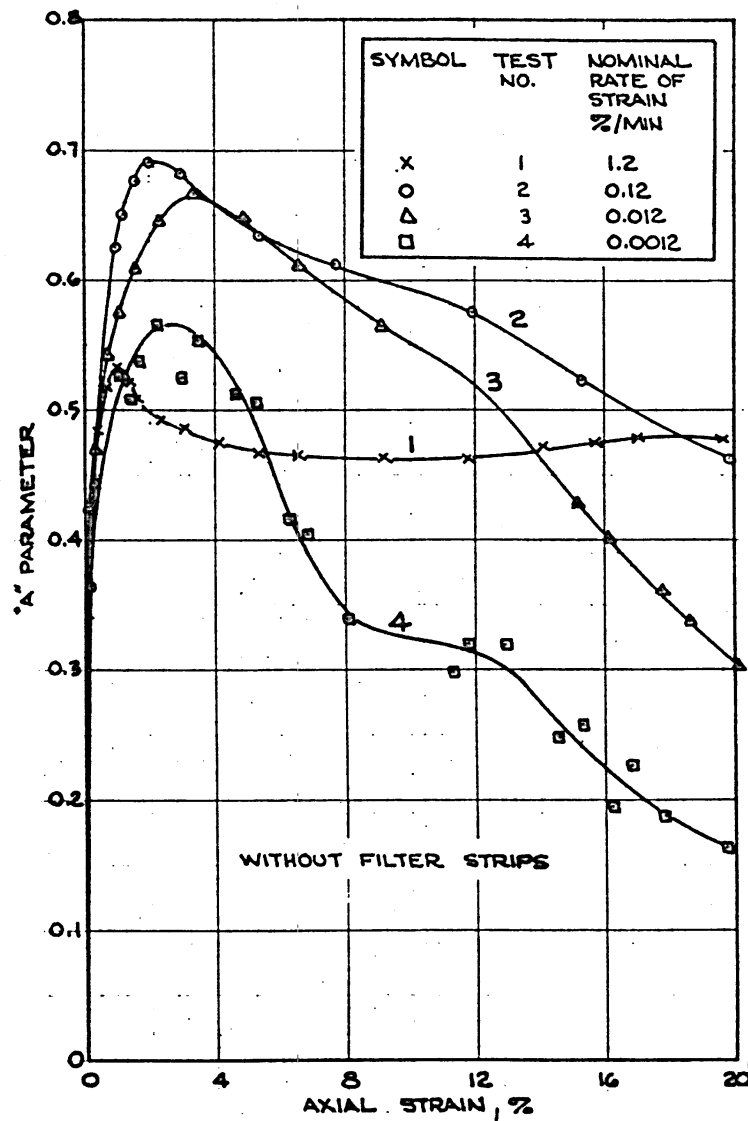


Fig. 11. Pore pressure parameter A versus axial strain,
 $\bar{\sigma}_c = 0.5 \text{ kg/sq cm}$

strain rates during the final part of shear. The probable reason for this behavior once again lies with end restraint. During the initial part of shear, greater shear strains in the middle of these specimens would produce a tendency for this portion of the specimens to consolidate more than the ends and pore pressures developed in this region would be higher than those measured at the bottom for the faster rates of strain. With decreased rates of strain, the pore pressure gradient would tend to dissipate and pore pressures measured at the bottom of the specimens would increase with decreasing strain rate. During the latter part of shear, however, the middle portion of the specimens would tend to dilate (see comparison of central water content to average water content in fig. 6), with the result that a decrease in induced pore pressure would occur with decreasing rates of strain for the final part of shear. There was no effect of the filter strips on observed pore pressures during the early part of shear as shown by the curves at 1 percent strain. At 15 percent strain, lower pore pressures were observed in tests with filter strips than in those without filter strips. Plots of A parameter versus axial strain for these tests are given in fig. 12.

Effective stresses

21. Plots of effective principal stress ratio ($\bar{\sigma}_1/\bar{\sigma}_3$) versus axial strain for the 0.5- and 5.0-kg-per-sq-cm tests are given in figs. 13 and 14, respectively. These figures show that axial strains at $\bar{\sigma}_1/\bar{\sigma}_3 \text{ max}$ for the tests at $\bar{\sigma}_c = 0.5$ kg per sq cm ranged from 1 to 4 percent and increased with decreasing rates of strain while those for the tests at $\bar{\sigma}_c = 5.0$ kg per sq cm ranged from 8 to 15 percent and decreased with decreasing strain rates. The very high peak values of the effective principal stress ratio in the tests at $\bar{\sigma}_c = 5.0$ kg per sq cm performed at 1.2 percent per minute are believed to result because the strain rate is too fast for reliable pore pressure measurement to be made at the base of the specimen. Plots of maximum principal stress ratio (or at 15 percent strain in the case of $\bar{\sigma}_c = 5.0$ kg per sq cm) versus elapsed time of shear are given in fig. 15. These plots indicate that values for specimens with and without filter strips fall on same curve after approximately 60 minutes for the 0.5-kg-per-sq-cm tests and approximately 120 minutes for the

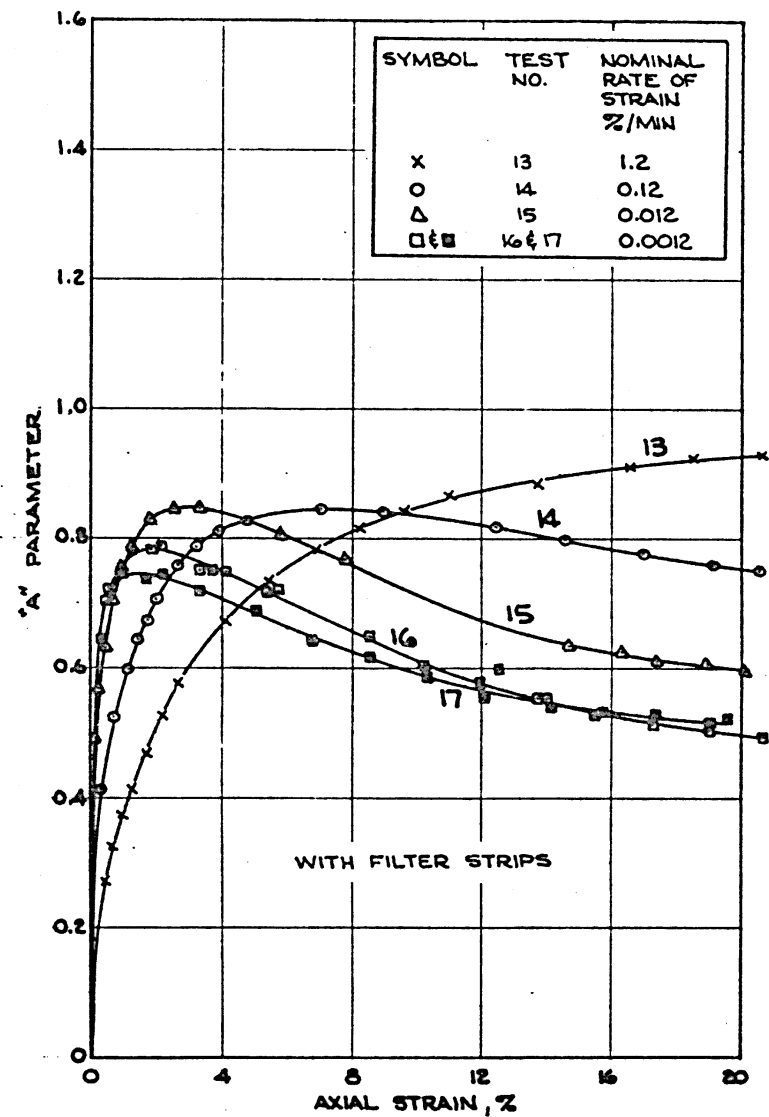
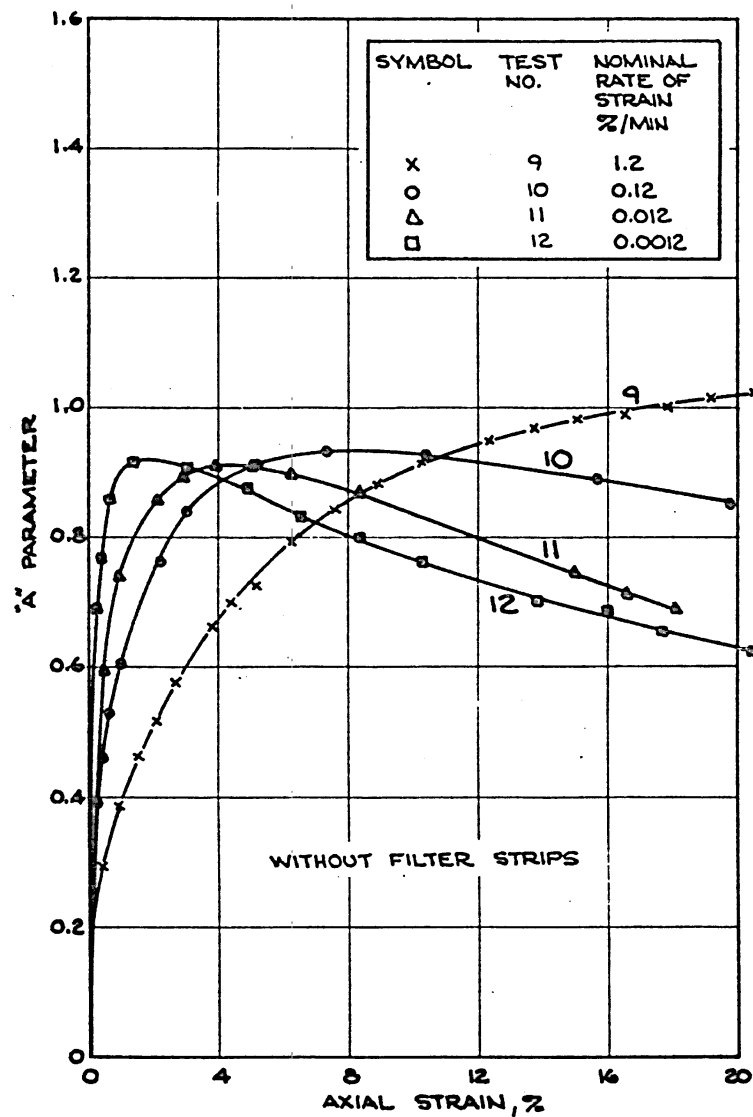


Fig. 12. Pore pressure parameter A versus axial strain,
 $\bar{\sigma}_c = 5.0 \text{ kg/sq cm}$

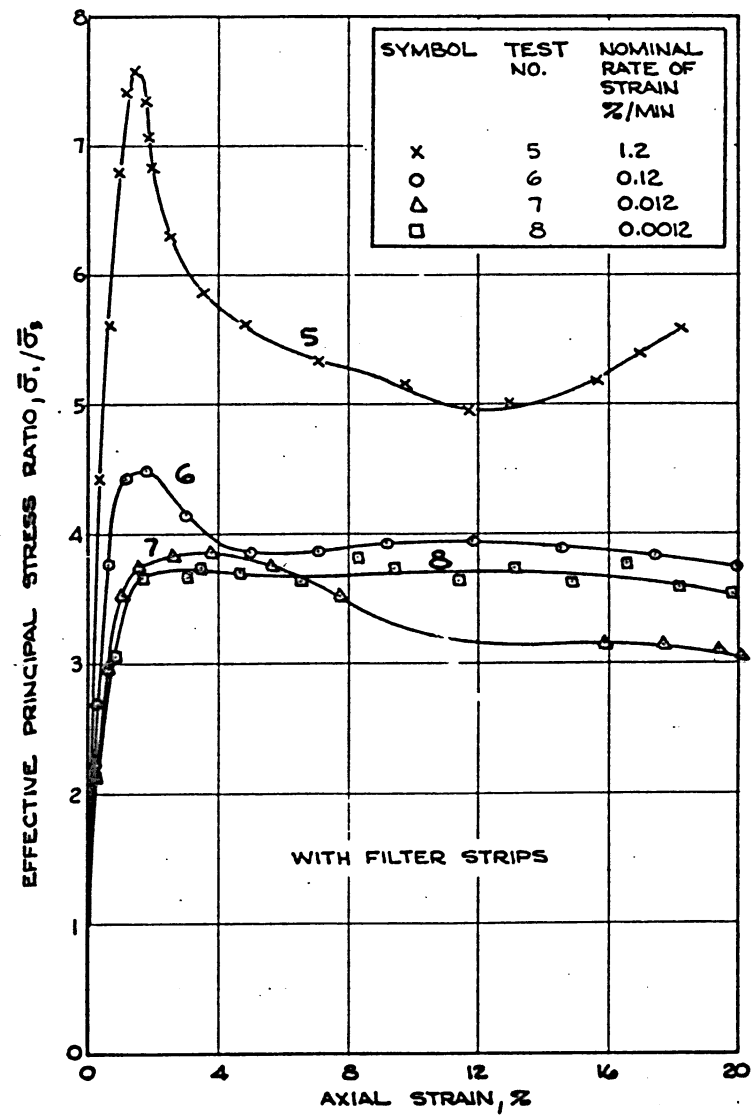
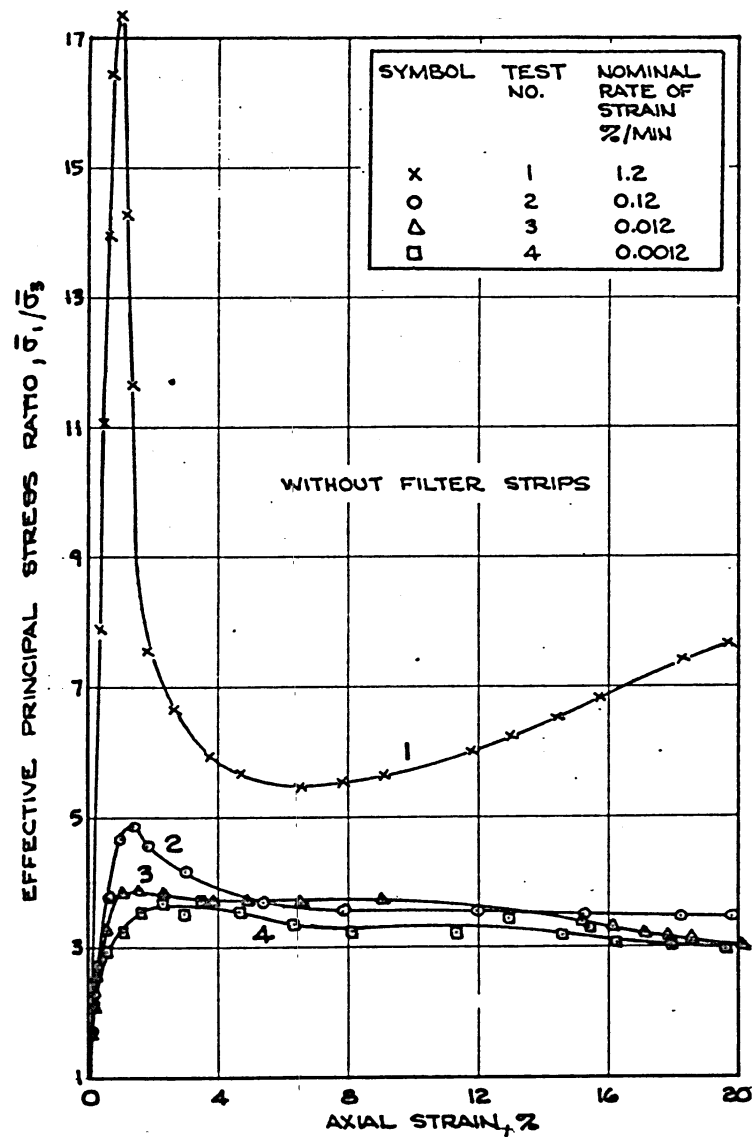


Fig. 13. Effective principal stress ratio versus axial strain,
 $\bar{\sigma}_c = 0.5 \text{ kg/sq cm}$

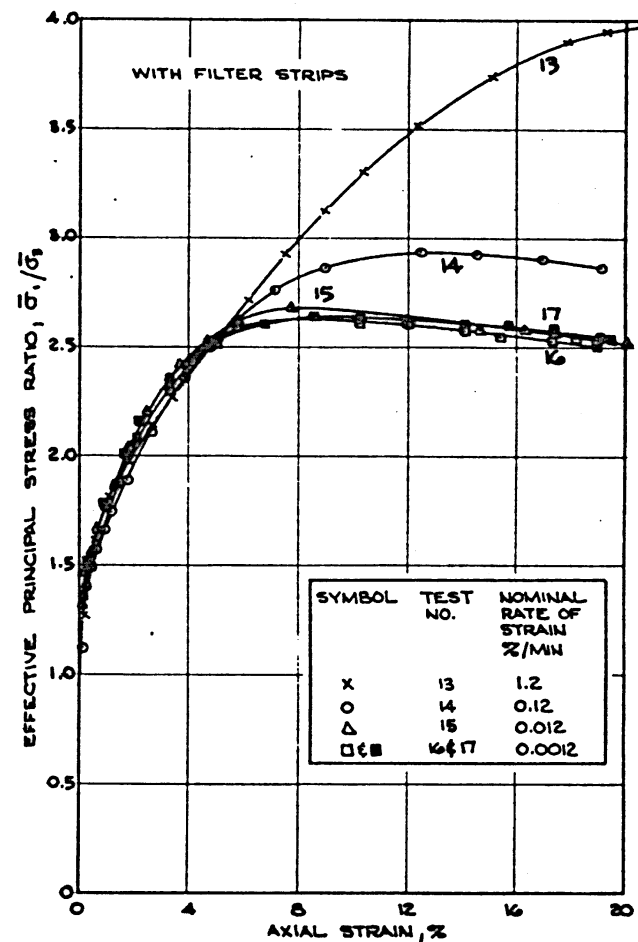
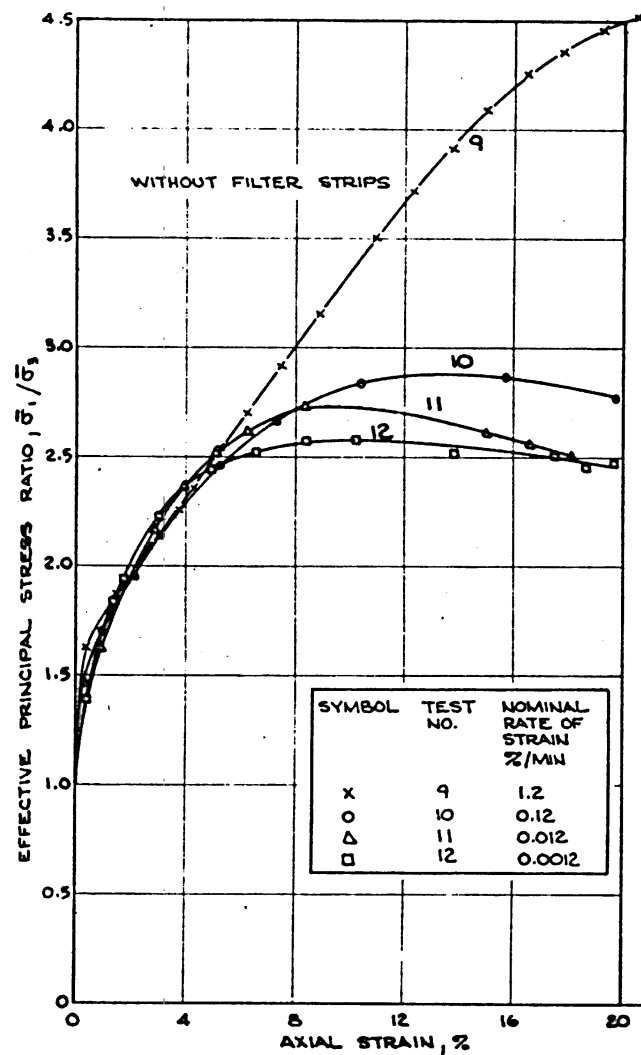


Fig. 14. Effective principal stress ratio versus axial strain, $\bar{\sigma}_c = 5.0 \text{ kg/sq cm}$

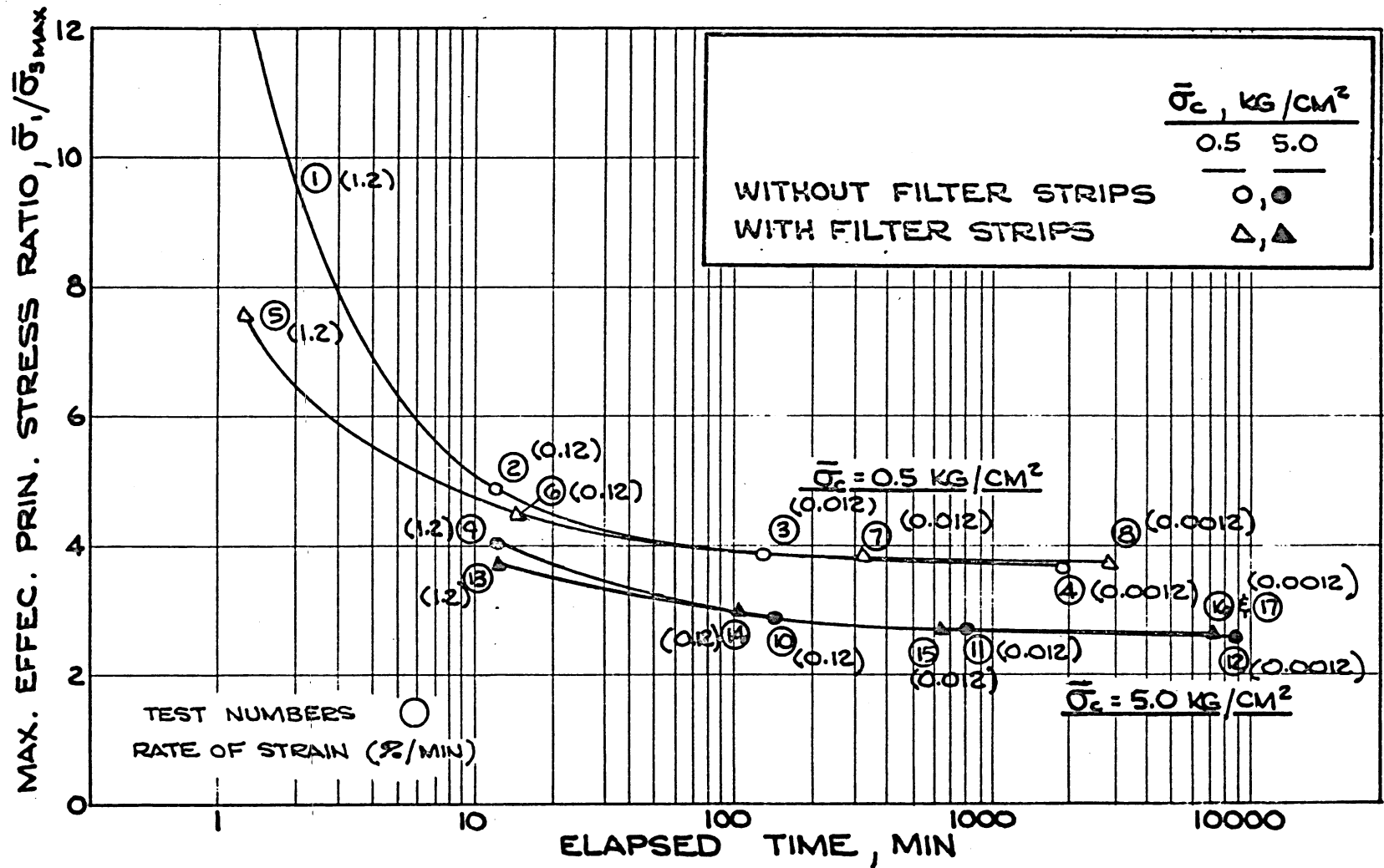


Fig. 15. Maximum principal stress ratio versus elapsed time of shear

5.0-kg-per-sq-cm tests. The curves become quite flat for longer times. The lowest maximum principal stress ratio for the normally consolidated specimens tested under $\bar{\sigma}_c = 0.5$ kg per sq cm was 3.70 and the lowest value for the specimens tested under $\bar{\sigma}_c = 5.0$ kg per sq cm was 2.60. Vector curves for effective stresses on 60-deg planes are given in figs. 16 and 17.

Influence of specimen deformation on deviator stresses

22. Although the plots of deviator stresses at 15 percent strain in figs. 8 and 10 indicate increases in deviator stresses with slower rates of strain, these increases possibly did not actually occur. As the rate of strain was decreased in the tests, the effects of end restraint became more pronounced with increased shear strains in the middle portions of the specimens and excessive bulging in this region (see failure sketches, figs. 4 and 5). Because of this localized bulging, the computation of deviator stresses using corrected areas based on the assumption that specimens remain cylindrical in shape during axial loading could be in considerable error. If excessive bulging is assumed to have occurred only in the middle half of the specimens as appeared to be the case for tests at the slowest rate of strain (0.0012 %/min), deviator stresses at 15 percent strain when computed in the normal way would be approximately 20 percent higher for the tests with the longest times of shear than if corrected areas were based only on central bulging. For the case of bulging only of the middle half, the cross-sectional area of the specimen used in computing the deviator stresses is defined by the equation:*

$$A'_{\text{corr}} = \frac{A_c}{1 - 2\epsilon} \quad (1)$$

where

A'_{corr} = corrected area after strain ϵ

A_c = area of specimen after consolidation

ϵ = strain

* The customary equation, assuming a cylindrical cross section throughout the height of the specimen, is:

$$A'_{\text{corr}} = \frac{A_c}{1 - \epsilon}$$

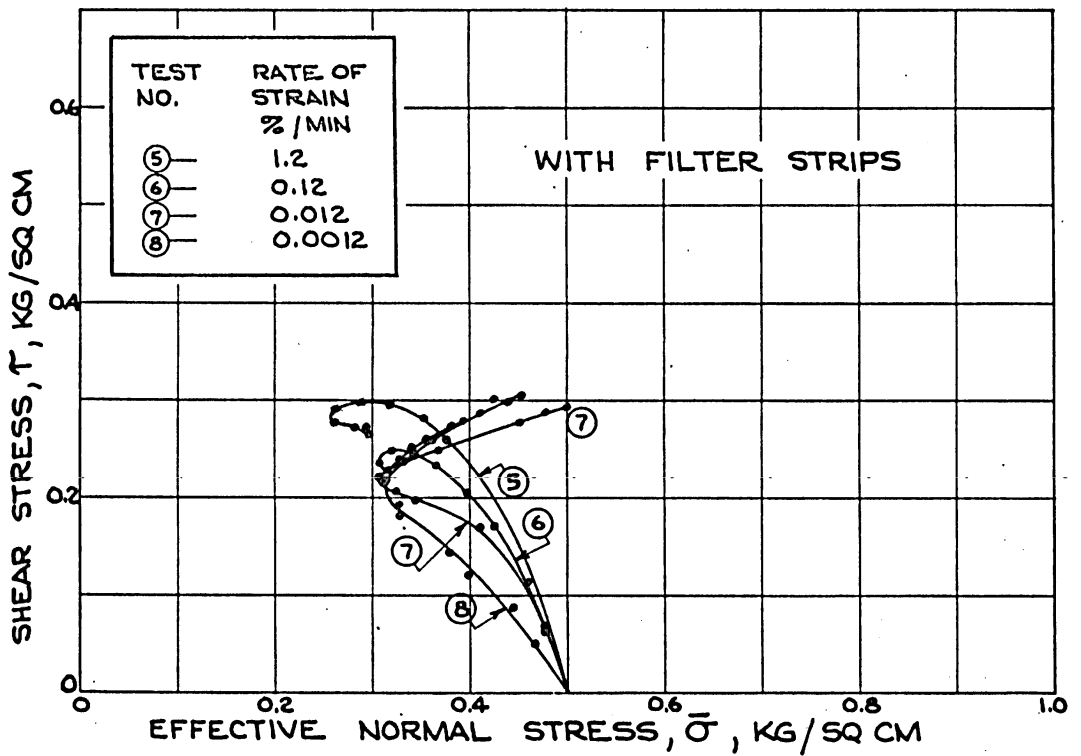
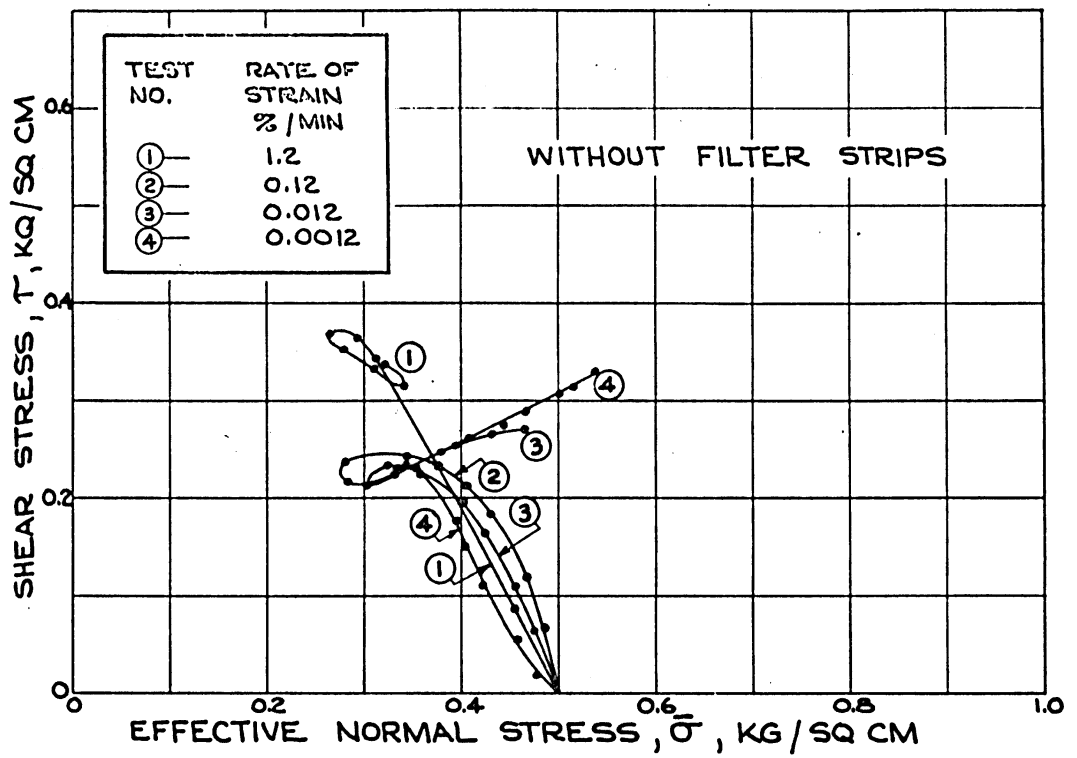


Fig. 16. Stress paths on 60-deg plane, $\bar{\sigma}_c = 0.5$ kg/sq cm

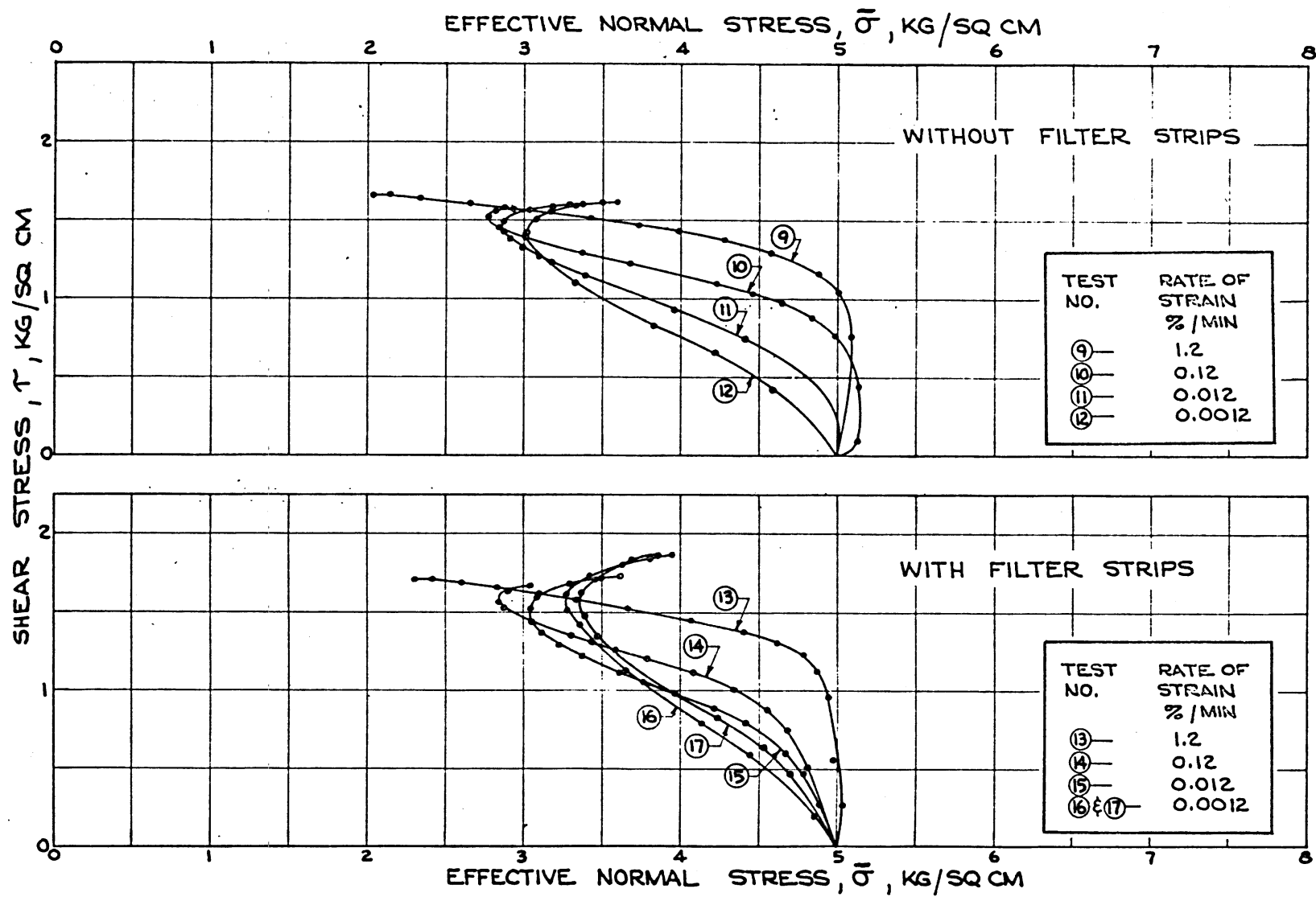
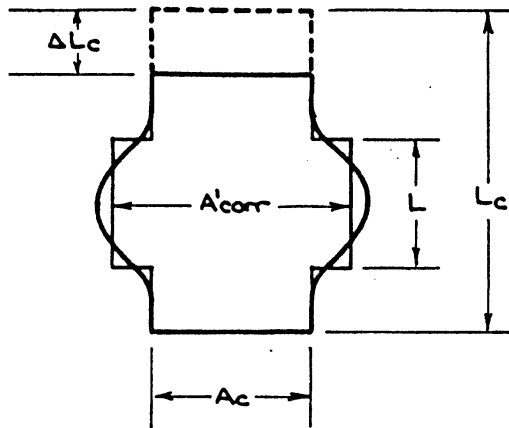


Fig. 17. Stress paths on 60-deg plane, $\bar{\sigma}_c = 5.0$ kg/sq cm

The derivation of equation (1) and the effects of corrections based on central bulging on deviator stresses are given in fig. 18.

23. For tests at $\bar{\sigma}_c = 0.5$ kg per sq cm, the computation of deviator stresses at failure would not be affected by use of the equation for central bulging since the failure points were at very low strains before any appreciable bulging had occurred. However the computation of deviator stresses at greater strains based on central bulging would change the shape of the stress-strain curves as shown in fig. 19 for test 8 performed at a rate of strain of 0.0012 percent per min. For the tests performed under $\bar{\sigma}_c = 5.0$ kg per sq cm, the maximum deviator stress at the slowest rate of strain is considerably changed. It is shown in fig. 19 for test 16 that the maximum deviator stress computed on the basis of bulging only in the central half of the specimen was 3.62 kg per sq cm versus 4.26 computed by the customary method.

24. Figure 20 is a plot of deviator stress at failure versus elapsed time to failure for all tests. The points in fig. 20 identified by circles and triangles are the same as those in figs. 8 and 10, representing deviator stresses computed by using the conventional area correction. The points identified by x's for tests at the slowest rate of strain represent deviator stresses computed on the basis of area corrections based on central bulging. The adjusted curves shown in fig. 20 are based on deviator stresses computed on the assumptions that (a) the conventional area correction is acceptable for tests performed at rates of strain of 1.2 and 0.12 percent per min (in which bulging was moderate and not particularly localized), and (b) the area correction for bulging of the central half is applicable for the tests run at the slowest rate of strain (0.0012 percent per min) in which central bulging was very pronounced. The curves for tests at $\bar{\sigma}_c = 0.5$ kg per sq cm are unaffected by the recomputation as deviator stresses at failure occurred at very small strains before appreciable bulging had taken place. The curves for tests at $\bar{\sigma}_c = 5.0$ kg per sq cm, however, now show a reduction of deviator stress at failure with decreasing rate of the shear. The following tabulation summarizes this reduction in deviator stress with increasing times to failure, using the adjusted



$$L = \frac{L_c}{2} - \Delta L_c$$

$$\text{since } \Delta L_c = \epsilon L_c$$

$$L = \frac{L_c}{2} - \epsilon L_c \quad \text{or}$$

$$L = \frac{L_c}{2} (1 - 2\epsilon)$$

$$A'_{\text{corr}} = \frac{V}{L} = \frac{A_c L_c}{2L}$$

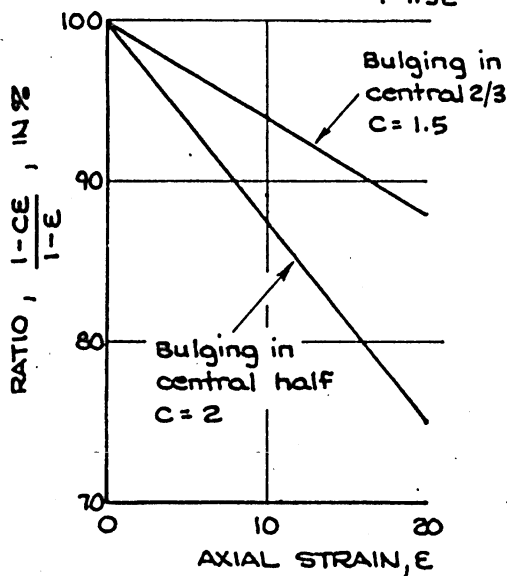
$$A'_{\text{corr}} = \frac{A_c L_c}{2} \div \frac{L_c (1 - 2\epsilon)}{2}$$

$$A'_{\text{corr}} = \frac{A_c}{1 - 2\epsilon}$$

DETERMINATION OF A'_{corr} WHEN BULGING IS CONFINED TO CENTRAL HALF OF SPECIMEN

For the case when bulging is confined to the central two-thirds of the specimen :

$$A'_{\text{corr}} = \frac{A_c}{1 - 1.5\epsilon}$$



$\frac{1 - CE}{1 - E}$ = ratio of area corrected using the usual assumption of a cylindrical cross section maintained during shear to the area corrected assuming localized central bulging. It is therefore the ratio of the deviator stresses based on localized bulging to those computed in the usual way.

Fig. 18. Effects of localized central bulging on computed deviator stresses

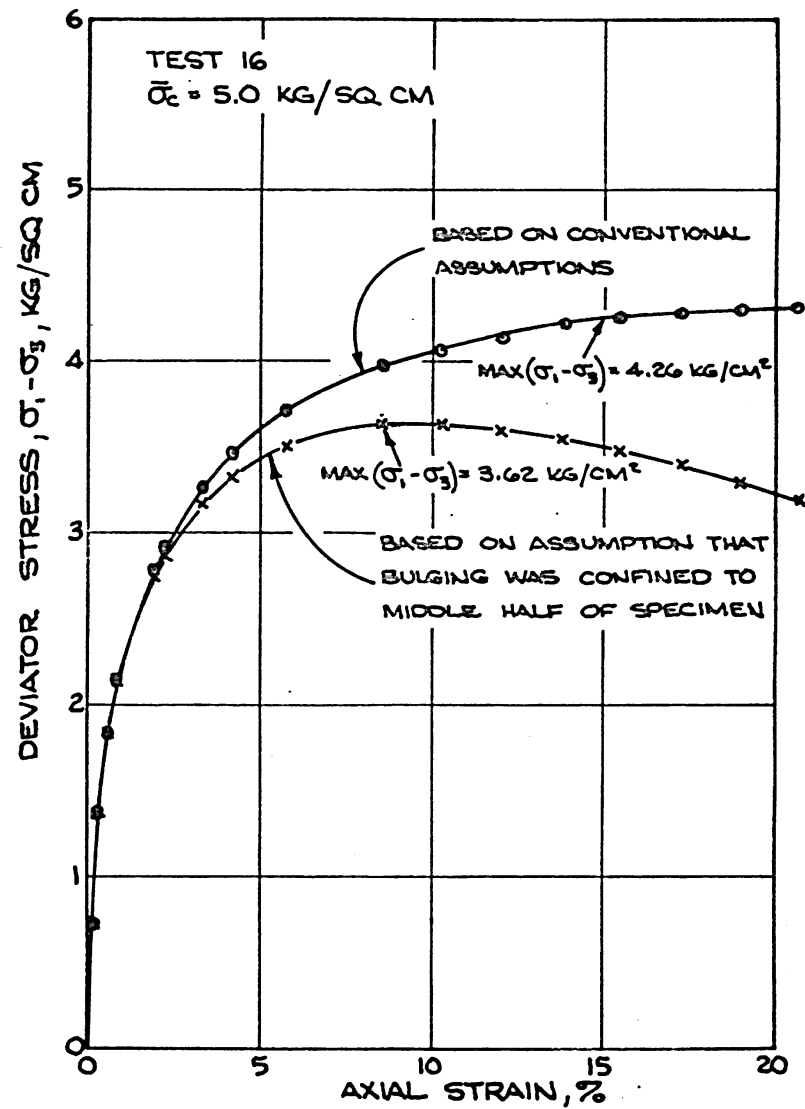
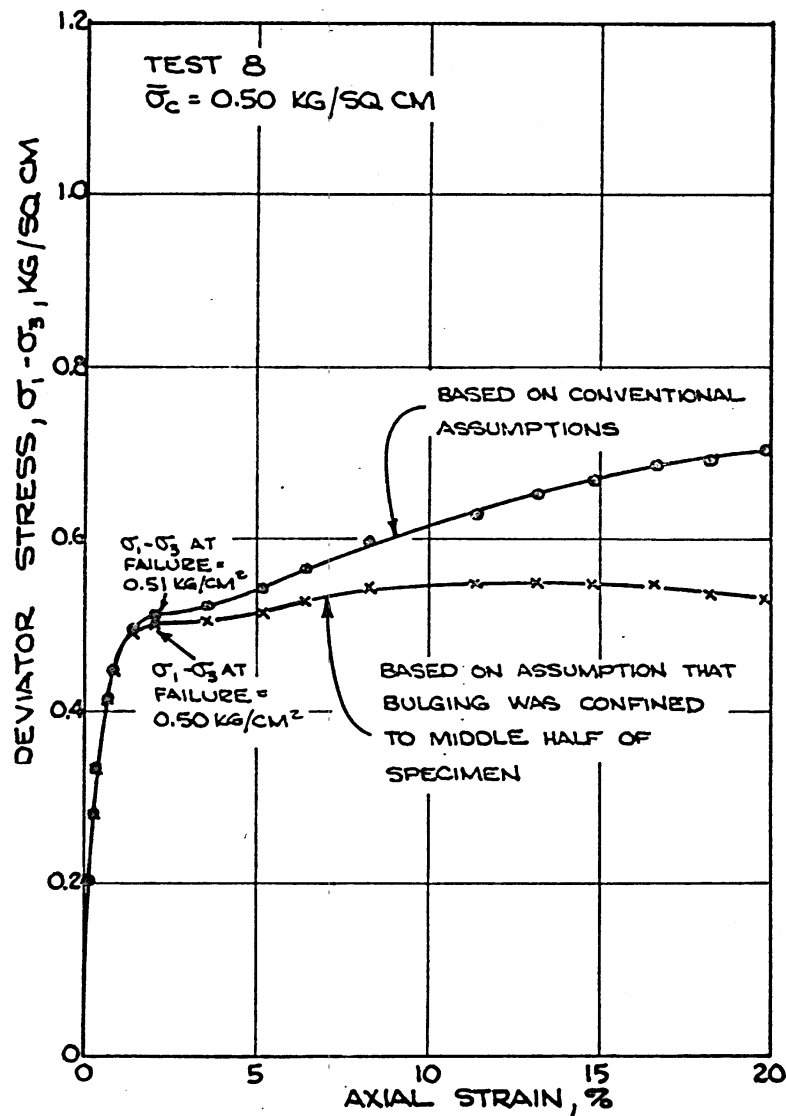


Fig. 19. Deviator stresses computed two ways versus axial strain; tests 8 and 16 with filter strips, rate of strain = 0.0012% per min

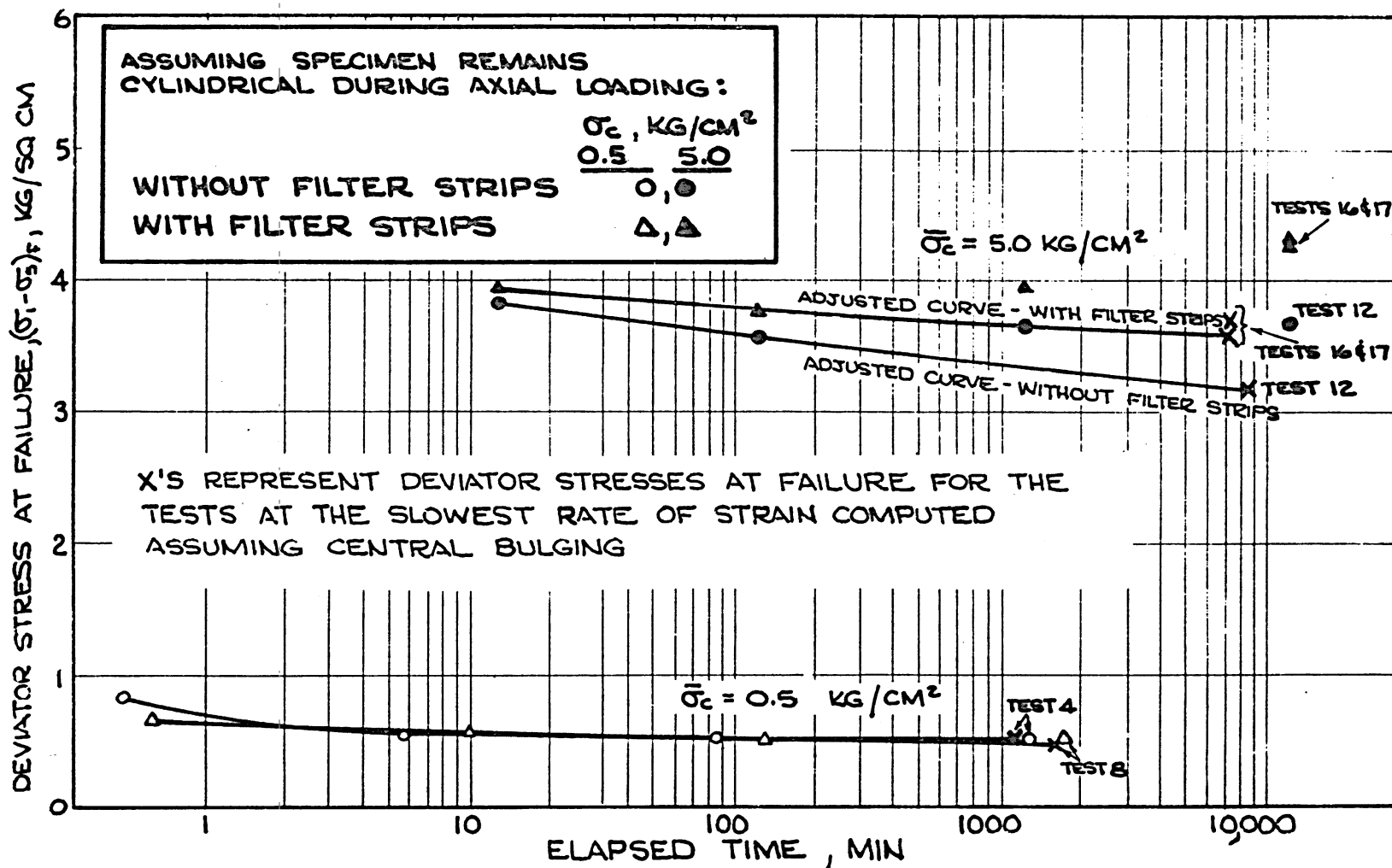


Fig. 20. Deviator stresses at failure versus elapsed time of shear

curves in fig. 20.

$\bar{\sigma}_c = 5.0 \text{ kg/sq cm}$	Rate of Strain, $\dot{\epsilon}$, %/min			
	1.2	0.12	0.012	0.0012
<u>With filter strips:</u>				
Time to failure, min	13	125	900	7167
Deviator stress, kg/cm^2	3.94	3.78	3.69	3.62
Deviator stress relative to value at $\dot{\epsilon} = 0.12 \text{ \%/min}$	1.04	1.00	0.98	0.95
<u>Without filter strips:</u>				
Time to failure, min	13	125	1000	3600
Deviator stress, kg/cm^2	3.83	3.58	3.36	3.18
Deviator stress relative to value at $\dot{\epsilon} = 0.12 \text{ \%/min}$	1.07	1.00	0.94	0.89

Based on the adjusted curves in fig. 20, the equation for the cross-sectional area of specimens sheared at the 0.012 percent per minute strain rate is:

$$A'_{\text{corr}} = \frac{A_c}{1 - 1.5\epsilon} \quad (2)$$

Strength envelopes

25. Mohr's circles and shear strength envelopes based on total stresses are shown in fig. 21. Solid lines and circles are based on conventional area corrections used to compute deviator stresses. The dashed Mohr's circles, labeled C' and D', are for deviator stresses computed using area corrections based on localized bulging in tests at $\bar{\sigma}_c = 5.0 \text{ kg per sq cm}$, and sheared at the two slowest rates of strain. The following tabulation shows the highest and lowest shear strength values

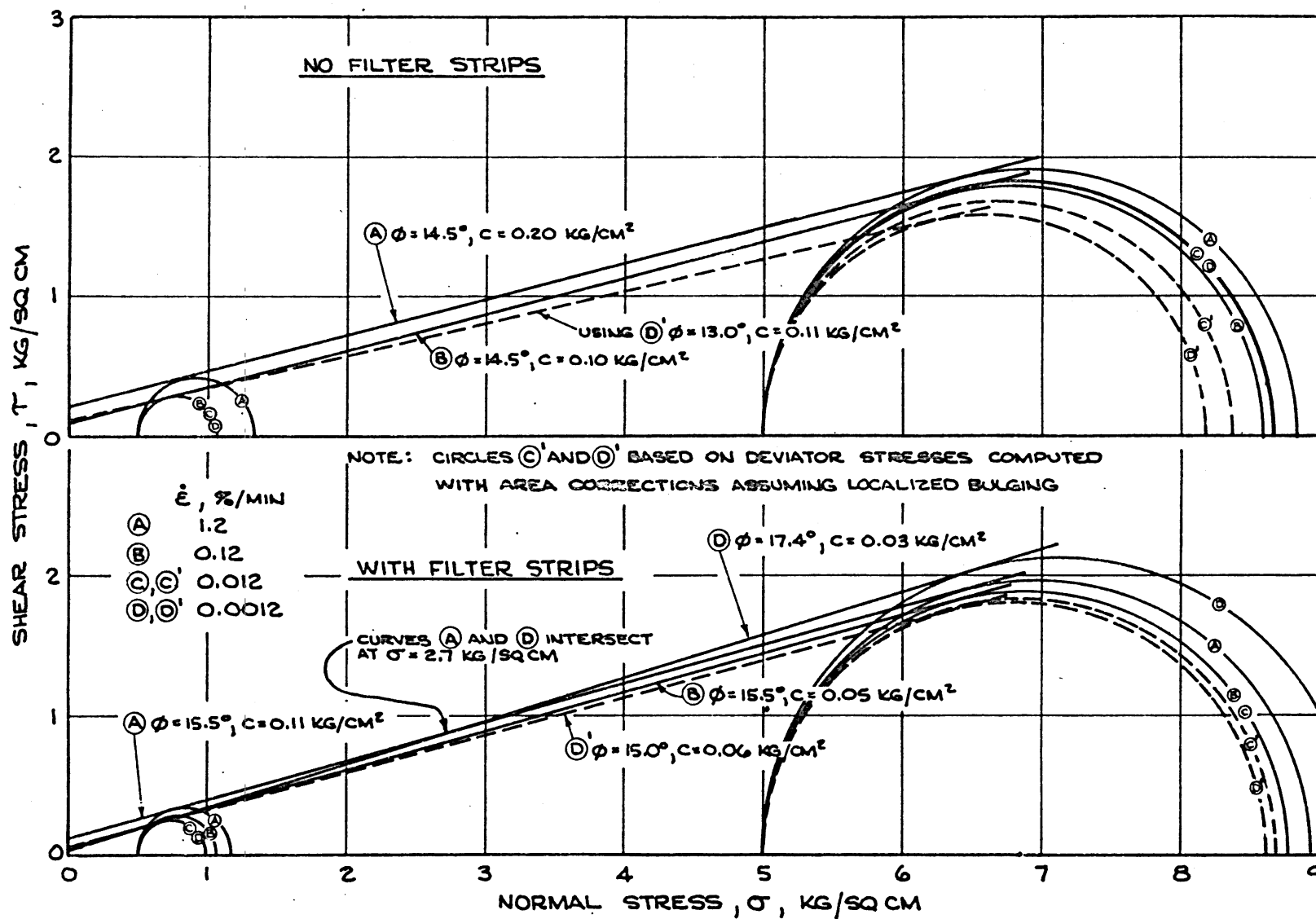


Fig. 21. Mohr's diagrams based on total stresses

taken from fig. 21:

Shear Strength Based on Total Stresses		
	ϕ deg	c kg/cm ²
1. <u>No filter strips:</u>		
<u>a. Highest shear strength</u>		
Rate of strain ($\dot{\epsilon}$) = 1.2 %/min	14.5	0.20
<u>b. Lowest shear strength</u>		
(1) Usual area correction		
$\dot{\epsilon} = 0.12$ %/min	14.5	0.10
(2) Central bulging correction		
$\dot{\epsilon} = 0.0012$ %/min	13.0	0.11
2. <u>With filter strips:</u>		
<u>a. Highest shear strength</u>		
(1) $\sigma > 2.7$ kg/cm ²		
$\dot{\epsilon} = 0.0012$ %/min	17.4	0.03
(2) $\sigma < 2.7$ kg/cm ²		
$\dot{\epsilon} = 1.2$ %/min	15.5	0.11
<u>b. Lowest shear strength</u>		
(1) Usual area correction		
$\dot{\epsilon} = 0.12$ %/min	15.5	0.05
(2) Central bulging correction		
$\dot{\epsilon} = 0.012$ and 0.0012 %/min	15.0	0.06
26. From fig. 21 and the above tabulation, it is indicated that:		
<u>a.</u> Total shear strengths for tests at $\bar{\sigma}_c = 5.0$ kg per sq cm are higher for specimens with filter strips than those without filter strips. For tests at $\bar{\sigma}_c = 0.5$ kg per sq cm, the reverse is true.		
<u>b.</u> At both $\bar{\sigma}_c$ values and for specimens both with and without filter strips, the shear strengths for tests at a rate of strain of 1.2 percent per min were considerably higher than		

those at slower rates except for the $\bar{\sigma}_c = 5.0$ kg per sq cm tests at 0.012 and 0.0012 percent per min, in which much centralized bulging occurred.

- c. If deviator stresses for the tests at $\bar{\sigma}_c = 5.0$ kg per sq cm run at the two slower rates of strain are computed using corrected areas based on localized bulging, the shear strengths are lower than for tests run at the two faster rates.

Summary and Conclusions

27. The use of filter strips appreciably reduced the times required for saturation of specimens, and for consolidation of specimens under $\bar{\sigma}_c = 5.0$ kg per sq cm: saturation times averaged 4 days for specimens with strips and 12 days without; consolidation times averaged 4 days for specimens with strips and 6 days without.

28. Deviator stresses at failure were somewhat greater for specimens without filter strips in tests with $\bar{\sigma}_c = 0.5$ kg per sq cm, and somewhat less for specimens with filter strips in tests with $\bar{\sigma}_c = 5.0$ kg per sq cm. The specimens tested at $\bar{\sigma}_c = 0.5$ kg per sq cm failed at low strains (0.7 to 2.1 percent), while stress-strain curves for tests at $\bar{\sigma}_c = 5.0$ kg per sq cm did not peak, and the maximum deviator stress was taken to be that at 15 percent strain.

29. Using the conventional method of correcting the cross-sectional area during axial strain in computing the deviator stress, deviator stresses at failure were lowest at rates of strain of 0.012 and 0.12 percent per min for tests at $\bar{\sigma}_c = 0.5$ and 5.0 kg per sq cm, respectively (times to failure of 133 and 125 min, respectively).

30. It was noted that bulging during axial loading at the two slower rates of strain was largely confined to the central portion of the specimen, most likely due to end restraint imposed by the standard caps and bases used. If deviator stresses were computed using corrected areas based on central bulging (see para 22), the resulting stress-strain curves (see fig. 19) show a slight reduction in deviator stress at failure for the

tests at $\bar{\sigma}_c = 5.0$ kg per sq cm with decreasing rate of strain rather than an increase in deviator stress for the two slowest rates of strain (fig. 20). Thus the conventional method of area correction appears to introduce considerable error in computations for deviator stresses for tests in which maximum deviator stresses are not reached until specimens have undergone large strains and excessive localized bulging. This suggests that low-friction caps and bases (oversize polished surfaces with small porous inserts) may be needed in R tests on specimens that fail at large strains.

31. Further research is required to investigate the effect of rate of strain on total shear strength with specimens sheared using low-friction caps and bases.

Unclassified

Security Classification

DOCUMENT CONTROL DATA - R & D

(Security classification of title, body of abstract and indexing annotation must be entered when the overall report is classified)

1. ORIGINATING ACTIVITY (Corporate author) U. S. Army Engineer Waterways Experiment Station Vicksburg, Mississippi		2a. REPORT SECURITY CLASSIFICATION Unclassified	
		2b. GROUP	
3. REPORT TITLE EFFECTS OF STRAIN RATE IN CONSOLIDATED-UNDRAINED TRIAXIAL COMPRESSION TESTS OF COHESIVE SOILS; Report 2, VICKSBURG BUCKSHOT CLAY (CH)			
4. DESCRIPTIVE NOTES (Type of report and inclusive dates) Report 2 of a series			
5. AUTHOR(S) (First name, middle initial, last name) Robert T. Donaghe			
6. REPORT DATE May 1971	7a. TOTAL NO. OF PAGES 45	7b. NO. OF REFS 2	
8a. CONTRACT OR GRANT NO.	9a. ORIGINATOR'S REPORT NUMBER(S) Miscellaneous Paper S-70-8, Report 2		
b. PROJECT NO.			
c.	9b. OTHER REPORT NO(S) (Any other numbers that may be assigned this report)		
d.			
10. DISTRIBUTION STATEMENT Approved for public release; distribution unlimited.			
11. SUPPLEMENTARY NOTES		12. SPONSORING MILITARY ACTIVITY Office, Chief of Engineers, U. S. Army Washington, D. C.	
13. ABSTRACT The results of consolidated-undrained (R) triaxial compression tests with pore pressure measurements performed to determine the effects of strain rate on the strength and deformation characteristics of Vicksburg buckshot clay (CH) are presented and analyzed in this report. The 1.4-in.-diam triaxial specimens were compacted with a Harvard miniature compactor to 95 percent of maximum dry density derived from the standard effort compaction test with water contents 2 percentage points wet of standard optimum. Standard caps and bases (having the same diameter as the test specimen, with 1-in.-diam rigid porous inserts and drainage connections) were used in the triaxial tests. After back-pressure saturation and consolidation under effective confining pressures of 0.5 and 5.0 kg per sq cm, specimens with and without filter strips were axially loaded at rates of strain varying from 1.2 to 0.0012 percent per minute. Data presented include stress-strain curves, pore pressure observations, final water content distributions within the specimens, and shear strength envelopes based on total stresses. The use of filter strips on the sides of the specimens appreciably reduced times required for saturation of all specimens and for consolidation of specimens under the effective pressures ($\bar{\sigma}_c$) of 5.0 kg per sq cm. Using the normal procedures for calculating deviator stresses, deviator stresses at failure were lowest at rates of strain of 0.012 and 0.12 percent per min for tests at $\bar{\sigma}_c = 0.5$ and 5.0 kg per sq cm, respectively. Times to failure for the two $\bar{\sigma}_c$ were similar (133 and 125 min, respectively). Specimens sheared under $\bar{\sigma}_c = 0.5$ kg per sq cm failed at axial strains ranging between 1 and 3 percent; specimens sheared under $\bar{\sigma}_c = 5.0$ kg per sq cm continued to have increasing deviator stress with increasing axial strain. Very localized bulging of specimens occurred in tests at the two slowest rates of strain; this bulging or barreling invalidates the assumption that the specimen remains cylindrical for its entire height during axial loading. The conventional method for computing specimen area at large axial strains is not applicable for specimens that exhibit excessive bulging. The use of low-friction caps and bases to reduce end restraint and minimize the tendency of some specimens to exhibit a bulging failure mode will be investigated, and results will be presented in a subsequent report. A modified method for computing specimen area during axial loading to take in account excessive bulging is discussed.			

DD FORM 1473
1 NOV 66REPLACES DD FORM 1473, 1 JAN 64, WHICH IS
OBSOLETE FOR ARMY USE.Unclassified
Security Classification

Unclassified

Security Classification

14.	KEY WORDS	LINK A		LINK B		LINK C	
		ROLE	WT	ROLE	WT	ROLE	WT
	Cohesive soils Compression tests Consolidated-undrained tests Pore pressure measurement Soil tests Triaxial compression tests Vicksburg buckshot clay						

Unclassified

Security Classification